tric properties of ferric hemoglobin derivatives reported in this volume by Di Iorio [4] might be explained on the same basis.

Time-resolved studies of the changes in the magnetic moment of iron on rebinding of carbon monoxide to human hemoglobin have been reported.[22]

[22] J. Philo, *Proc. Natl. Acad. Sci. U.S.A.* **74,** 2620 (1977).

[22] Resonance Raman Spectroscopy of Hemoglobin

By SANFORD A. ASHER

Resonance Raman spectroscopy is almost an ideal probe of heme geometry and bonding in hemoglobin and myoglobin.[1–4] The technique selectively examines molecular bonding in and around the heme, the iron, and its ligands and is sensitive to bond length changes of less than 0.001 Å and to heme macrocycle electron density changes of less than 0.1 electrons. The technique is ideally suited for aqueous protein solutions at concentrations variable from the physiological heme concentration in the red blood cell to the submicromolar level. The technique is also easily utilized for single-crystal protein studies or for studies of model heme complexes in organic solution or in the form of the single crystals used for X-ray diffraction structural determinations.

Resonance Raman investigations of heme protein structure, function, and mechanism rapidly advanced after the first observation of the resonance Raman spectra of hemoglobin by Strekas and Spiro reported in 1972.[5] The critical components necessary for progress in the the field, advances in Raman theory, empirical data on model heme complexes, advances in instrumentation, and data on hemoglobin and myoglobin derivatives were all in phase. This resulted in progressively more incisive studies of heme structure, ligand bonding, and heme–globin interactions. More recently, kinetic resonance Raman photolysis measurements of carbon monoxyhemoglobin ($Hb^{II}CO$) in the picosecond and nanosecond time regimes[6–11a] appear to have temporally separated the heme structural and

[1] T. G. Spiro, in this series, Vol. 14, p. 233.
[2] N.-T. Yu, *CRC Crit. Rev. Biochem.* **4,** 229 (1977).
[3] A. Warshel, *Annu. Rev. Biophys. Bioeng.* **6,** 273 (1977).
[4] D. L. Rousseau, J. M. Friedman, and P. F. Williams, *Top. Curr. Phys.* **11,** 203 (1979).
[5] T. C. Strekas and T. G. Spiro, *Biochim. Biophys. Acta* **263,** 830 (1972).
[6] W. H. Woodruff and S. Farquharson, *Science* **201,** 831 (1978).
[7] J. M. Friedman and K. B. Lyons, *Nature* (*London*) **284,** 570 (1980).

METHODS IN ENZYMOLOGY, VOL. 76

ISBN 0-12-181976-0

ligand bonding changes resulting from the movement of the iron from the heme plane upon formation of 5-coordinate deoxyhemoglobin, from tertiary subunit structural changes and the tetramer quaternary structural changes. These studies will be fundamental for elucidation of the molecular mechanism of hemoglobin cooperativity.

The advances in the resonance Raman technique over the last few years have been phenomenal. The harvesting of these advances in terms of an understanding of hemoglobin cooperativity is beginning to present new reliable data on the heme conformational dependence upon protein structure. Some of the results are consistent with previous studies using other techniques while other resonance Raman results have presented data which have challenged the present models for hemoglobin cooperativity. Hemoglobin is a very complex molecule and does not yield its secrets easily.

The Raman Phenomenon

Phenomenological Description of Raman Scattering

Resonance Raman spectroscopy, like normal Raman spectroscopy, results from the inelastic scattering of light from molecules.[12] In the case of vibrational Raman scattering, which is used for heme protein studies, the molecular quantum levels that exchange energy with the photon are vibrational energy levels. Thus the photon frequency shifts observed for Raman scattering correspond to molecular vibrational frequencies. The Raman spectral data are displayed in a manner similar to infrared (IR) spectra; the abscissa is labeled in units of cm^{-1}, and the ordinate corresponds to the scattered light intensity. The abscissa $\Delta\nu$ (cm^{-1}) values correspond to the magnitude of the frequency shift of the Raman peak from the frequency of the exciting light.

Figure 1 shows a diagrammatic representation of the Raman scattering

[8] K. B. Lyons, J. M. Friedman, and P. A. Fleury, *Nature (London)* **275,** 565 (1978).

[9] K. B. Lyons and J. M. Friedman, *in* "Interaction between Iron and Proteins in Oxygen and Electron Transport" (C. Ho, W. A. Eaton, J. P. Collman, Q. H. Gibson, J. S. Leigh, Jr., E. Margoliash, J. K. Moffat, and W. R. Scheidt, eds.). Elsevier, Amsterdam, 1981, in press.

[10] R. F. Dallinger, J. R. Nestor, and T. G. Spiro, *J. Am. Chem. Soc.* **100,** 6251 (1978).

[11] J. Terner, T. G. Spiro, M. Nagumo, M. F. Nicol, and M. A. El-Sayed, *J. Am. Chem. Soc.* **102,** 3238 (1980).

[11a] J. Terner, J. D. Strong, T. G. Spiro, M. Nagumo, M. Nichol, and M. A. El-Sayed, Proc. Natl. Acad. Sci. U.S.A. **78,** 1313 (1981).

[12] J. A. Koningstein, *in* "Introduction to the Theory of the Raman Effect." Reidel, Dordrecht, The Netherlands, 1972.

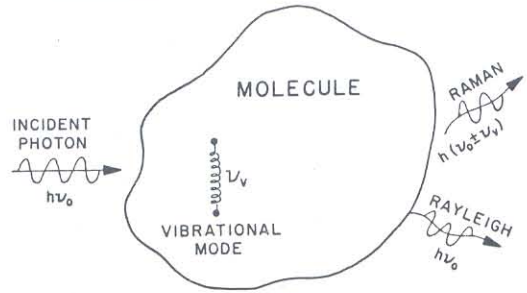

FIG. 1. Classical picture of the Raman scattering phenomenon.

mechanism; light from a laser at a frequency ν_0 induces oscillation in the electron cloud of a molecule. These oscillations occur at frequency ν_0, and their amplitude is proportional to the molecular polarizability at ν_0 (vide infra). The resulting oscillating molecular dipole moment will radiate light of frequency ν_0; this phenomenon is called Rayleigh scattering.

Other dynamical molecular processes can couple to the polarizability to modulate the frequency and amplitude of the oscillating induced dipole moment. A molecular vibration represented by the spring with frequency ν_v in Fig. 1 can couple to the oscillating dipole moment, resulting in a beating of these oscillations with one another. This interaction results in frequency components at $\nu_0 \pm \nu_v$. Thus, light shifted by molecular vibrational frequencies will be radiated (Raman effect). This process is a scattering phenomenon and does not involve the consecutive absorption and reemission of photons.

From conservation of energy considerations Raman scattering at $\nu_0 + \nu_v$ (anti-Stokes) requires the molecule to exist initially in an excited vibrational level at least ν_v above its ground state. For normal temperatures and for vibrational frequencies >300 cm^{-1}, the population of excited-state molecules is small and most of the Raman intensity occurs within the Stokes region at $\nu_0 - \nu_v$.

The exciting laser light is both monochromatic and polarized in a specific direction with respect to the optical detection system that monitors the Raman scattered light. The resulting Raman spectra display frequency shifts that are sensitive to molecular bonding, which depends upon the molecular structure as it is influenced by the chemical environment. The resonance Raman intensities depend upon the ground and excited electronic states of the molecule and how these states interact with the vibrational modes. The final polarization of the Raman scattered light depends upon the symmetry of the molecule and the particular vibrational mode observed; the polarization of the Raman scattered light can be used to assign the observed vibrational Raman peaks. Polarization measurements

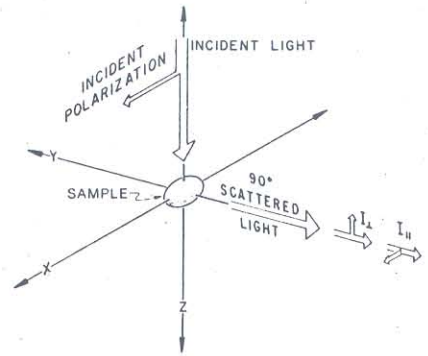

FIG. 2. Scattering geometry for depolarization ratio measurements.

are usually defined in terms of the depolarization ratio, $\rho = I_\perp/I_\parallel$, where, for one Raman peak, $I_\parallel$ and $I_\perp$ are the scattered intensities polarized parallel and perpendicular to the polarization of the exciting laser beam (Fig. 2).

The observed intensity I_v of the Raman scattered light at frequency $\nu_o - \nu_v$ depends linearly upon the incident laser intensity, I_o, and the number of scatterers, N:

$$I_v = K(\nu_o - \nu_v)^4 N I_o |\alpha_v|^2 \tag{1}$$

where K is a constant. The intensity depends upon the fourth power of the scattered frequency and upon a parameter α_v, which is the Raman polarizability tensor for the vibration at frequency ν_v. α_v specifies the coupling between the molecular vibration and the molecular polarizability at frequency ν_o. Classically the molecular polarizability can be expanded in the form

$$\alpha = \alpha_o + \frac{\partial \alpha}{\partial Q_v} dQ_v + \cdots \tag{2}$$

where the Raman polarizability is

$$\alpha_R{}^v = \frac{\partial \alpha}{\partial Q_v} dQ_v \tag{3}$$

and Q_v is the vibrational atomic displacement coordinate. The intensity of Raman scattering is specified when the value of $\alpha^v{}_R$ is known for each vibrational mode, v. The Raman intensities depend upon the electronic and vibrational states of the molecule. These states, in turn, depend upon molecular environment. Thus, intensity measurements for different vibrational modes can be used as a structural probe.

Excitation of the Raman spectra in resonance with an electronic transition results in a dramatic increase in the Raman scattered intensity,

often by as much as six orders of magnitude. This enhancement results from the fact that resonance excitation drives the molecular polarizability at its natural frequency, resulting in an increased amplitude for the oscillating dipole moment and a dramatically increased radiated intensity. The exact magnitude of enhancement for a particular vibrational mode depends upon its coupling to the resonant electronic transition. This dependency can be used to selectively observe particular vibrational modes by exciting the Raman spectra within particular electronic transitions coupled to those vibration.

Because of the absorption spectral shifts commonly occurring between different liganded complexes of hemoglobin, one can selectively examine individual species by exciting within the absorption spectral region specific for each complex. For example, the individual resonance Raman spectra of deoxyHb or Hb^{II}CO can be selectively examined with excitation at either 4150 Å or 4350 Å, respectively.[7]

The Raman Polarizability Tensor

For practical experimental considerations as well as for the potential molecular information available, it is important to relate the observed Raman intensities to molecular parameters. For hemoglobin resonance Raman studies this will require an understanding of the heme vibrational and electronic states as well as the Raman polarizability tensor.

The simplest form of the polarizability tensor relating the effect of the incident exciting light electromagnetic field at frequency ν_o on the electronic and vibrational states of the molecule is given[13–16] by

$$\alpha_R = A + B \tag{4}$$

$$A = \frac{1}{h} \sum_v \frac{\langle g|\rho|e\rangle\langle e|\sigma|g\rangle}{(\nu_e - \nu_g) - \nu_o + i\Gamma} \langle i|v\rangle\langle v|j\rangle \tag{5}$$

$$B = -\sum_s \sum_v \left[\langle g|\sigma|e\rangle \left\langle e\left| \frac{\partial H_e}{\partial Q_v} \right| s \right\rangle \langle s|\rho|g\rangle + \langle g|\rho|e\rangle \left\langle e\left| \frac{\partial H_e}{\partial Q_v} \right| s \right\rangle \langle s|\sigma|g\rangle \right] \times \frac{\langle i|Q_v|j\rangle}{(\nu_e - \nu_s)(\nu_e - \nu_g - \nu_o + i\Gamma)} \tag{6}$$

where g and e represent the molecular ground and resonant excited state,

[13] A. C. Albrecht and M. C. Hutley, *J. Chem. Phys.* **55,** 4438 (1971).
[14] A. C. Albrecht, *J. Chem. Phys.* **33,** 156 (1960).
[15] A. C. Albrecht, *J. Chem. Phys.* **34,** 1476 (1961).
[16] R. J. H. Clark and B. Stewart, *Struct. Bonding (Berlin)* **36,** 1 (1979).

and s represents another excited state. ρ and σ are the cartesian dipole moment operators defined in the molecular reference frame. The various combinations of σ and ρ occurring of the polarizability tensor specify the relationship between the intensity of Raman scattering with a polarization ρ, induced by the exciting light of polarization σ. Both σ and ρ are defined in terms of a specific orientation of the molecule with respect to incident and scattered light polarization. The depolarization ratio is theoretically determined from these components after they are appropriately averaged to account for the orientational averaging that occurs when a molecule is in solution.

The states $|i\rangle$, $|j\rangle$, and $|v\rangle$ represent vibrational wavefunctions, where $|v\rangle$ is a vibrational level of normal mode Q_v in the excited electronic state $1e\rangle$, while $|j\rangle$ and $|i\rangle$ are the initial and final vibrational levels of the ground electronic state. The subscripts on the frequency factors label the frequency of light necessary to induce an electronic transition from the ground state to the specified excited state. Γ is a parameter related to the lifetime of the resonant excited state. $\partial H_e/\partial Q_v$ is the Herzberg–Teller perturbation term reflecting the change in the electronic Hamiltonian that results from the vibrational displacement from equilibrium, occurring during the vibration of the normal mode Q_v.

Equations (4)–(6) indicate that Raman intensity derives from two mechanisms. The A term results from Franck–Condon overlap factors between the ground and excited states, $\langle i|v\rangle\ \langle v|j\rangle$. The intensity depends on this factor as well as on the transition moments $\langle e|\sigma|g\rangle$, and the frequency factors in the denominator. When the exciting frequency ν_0 approaches that necessary for an electronic excitation from the ground state to an excited state $|e\rangle$, ν_e the denominator becomes small, resulting in an dramatically increased Raman intensity. A-term enhancement is roughly proportional to the square of the extinction coefficient for absorption to the resonant excited $|e\rangle$.

The Stokes Raman process results in a vibrational transition from an initial vibrational sublevel i of vibration Q_v to a level $j = i + 1$. Both vibrational levels occur within the ground electronic state. This transition occurs via Franck–Condon overlaps through the vibrational level $|v\rangle$ of the excited electronic state. If identical vibrational states exist in the excited and ground states, no Raman scattering can occur via the A term. However, because electronic transitions are often accompanied by shifts in molecular geometry in the excited state relative to the ground state, the excited and ground vibrational wavefunctions are not solutions to the same molecular Hamiltonian. Thus, Raman scattering occurs with an intensity related to the shift in the molecular equilibrium geometry between the ground and excited electronic states. The A term picks out vibrational

modes whose atomic displacements occur along molecular coordinates that differ between the ground and excited states. For example, in a heme protein if the bond length between an axial ligand and the iron changes between the ground and excited states, enhancement of the iron–ligand stretch could occur via the A term. A-term enhancement of heme macrocyclic vibrational modes is frequently observed with excitation in the Soret band.[17] The vibrational modes enhanced by the A term are generally symmetric vibrations with low values of the Raman depolarization ratio and are called polarized.[16]

B term enhancement results from vibronic borrowing of intensity between the resonant electronic transition and an adjacent electronic transition. A description of the electronic states of a molecule in the absence of vibrations results in a set of states defined at the equilibrium internuclear separation. Molecular vibrations perturb these states to first order via the Herzberg–Teller ($\partial H_e/\partial Q_v$) perturbation matrix element occurring in the B term [Eq. (6)]. Thus, B-term enhanced vibrations are those coupling different electronic excited states and the vibrational modes enhanced are generally active within the resonant absorption band.

B term enhancement dominates the resonance Raman scattering of heme proteins excited within the α and β absorption bands.[18] This results from the significant contribution to the α and β absorptivity, which is due to vibronic borrowing of intensity from the Soret band. The symmetries of the allowed vibrational modes enhanced by the B term are those for which a totally symmetrical representation occurs in the cross product $\Gamma_s \times \Gamma_e \times \Gamma_Q$ from the $\langle s/\partial H_e/\partial Q_v|e\rangle$ matrix element. Since the excited states reached by absorption in the Soret and α and β bonds are of E_u symmetry, the allowed vibrational symmetries are $\Gamma_{E_u} \times \Gamma_{E_u} = A_{1g} + A_{2g} + B_{1g} + B_{2g}$. These vibrational symmetries result in depolarization ratios of $\rho = <0.75, \infty, 0.75, 0.75$, respectively.

The selection rule permitting vibrational Raman intensity is the matrix element $\langle j|Q_v|i\rangle$. This matrix element permits a change of one vibrational quantum for the vibrational mode Q_v during the Raman scattering process.

Resonance Raman studies of metalloporphyrins also indicate the existence of other mechanisms that can determine the magnitude of resonance Raman enhancement. Nonadiabatic effects[19,20] resulting from a breakdown of the separability of nuclear and electronic wavefunctions in the

[17] T. C. Strekas and T. G. Spiro, *J. Raman Spectrosc.* **1**, 197 (1973).
[18] T. G. Spiro, *Biochim. Biophys. Acta* **416**, 169 (1975).
[19] J. M. Friedman and R. M. Hochstrasser, *Chem. Phys.* **1**, 456 (1973).
[20] J. A. Shelnutt, D. C. O'Shea, N.-T. Yu, L. D. Cheung, and R. H. Felton, *J. Chem. Phys.* **64**, 1156 (1976).

Born–Oppenheimer approximation, as well as Jahn–Teller distortions[21] of degenerate excited states of the heme, can lead to more complex behaviors for Raman intensities.

The Raman intensity expressions in Eqs. (5) and (6) are relatively complex, and their quantitative use requires an understanding of the heme molecular vibrations and electronic transitions. Fortunately, the high effective symmetry of the heme, as well as the fact that the electronic structure can be treated in terms of relatively simple π molecular orbital theory, has permitted significant progress in the theoretical and experimental understanding of the heme visible and near-ultraviolet (UV) electronic transitions.[22,23]

From this work it appears that the visible and near-UV α, β, and Soret absorption bands result from electronic excitation from a nondegenerate ground state to two doubly degenerate excited states of E_u symmetry. These excited states are mixed by configuration interaction to result in an intense Soret absorption band between 4000 and 4500 Å and a less intense α band. The β band is the 0–1 vibronic overtone of the α band. Additional absorption features occur for many heme protein derivatives. For example, the ca 6000–6400 Å absorption features in Met derivatives of hemoglobin have been assigned to charge transfer transitions,[23] where electronic excitation involves transfer of electron density between heme macrocyclic molecular orbitals and iron *d* orbitals. Other charge transfer transitions can occur between the axial ligand and the iron, and between an axial ligand and the heme macrocycle.

Each of the scattering mechanisms, the *A* term, *B* term, nonadiabatic coupling, and Jahn–Teller distortions result in distinctly different excitation frequency intensity dependencies. These dependencies are examined by excitation profile measurements that monitor the resonance Raman intensity of a peak as the excitation frequency is tuned through an absorption band. Excitation profile measurements can also be used to resolve complex absorption spectra into separate overlapping electronic transitions. Because the excitation profiles of different Raman peaks are often sharply peaked at different positions within an absorption band, a knowledge of the excitation profiles permits the experimentalist to select an excitation frequency to maximally enhance a vibration of interest.

[21] J. A. Shelnutt, L. D. Cheung, R. C. C. Chang, N.-T. Yu, and R. H. Felton, *J. Chem. Phys.* **66**, 3387 (1977).
[22] D. W. Smith and R. J. P. Williams, *Struct. Bonding (Berlin)* **7**, 1 (1970).
[23] M. Zerner, M. Gouterman, and H. Kobayashi, *Theor. Chim. Acta* **6**, 363 (1966).

Experimental Considerations

Instrumentation

A typical resonance Raman spectrometer designed for signal averaging is shown in Fig. 3. The essential components include a laser source to excite the Raman scattering, a monochromator to analyze the frequencies of the scattered light, and an electronic detection system to detect the photon flux. A dye laser is essential in resonance Raman spectroscopy to measure excitation profiles and to select excitation frequencies to maximally enhance particular vibrational modes. The dye laser in Fig. 3 is a Coherent Radiation Model 490 jet stream dye laser, which is pumped by a high-power Model 171 Spectraphysics Ar^+ laser. This particular configuration permits a number of discrete excitation wavelengths between 4579 and 4880 Å and completely tunable excitation wavelengths between 4900 and 8000 Å.

Other lasers, such as the pulsed Chromatix CMX-4 flashlamp-pumped dye laser or the Molectron nitrogen laser-pumped dye laser, are tunable essentially throughout the visible spectral region. With frequency doubling these lasers are tunable in the UV. The pulsed lasers typically operate with pulse repetition rates between 10 and 100 Hz and with an equivalent CW average laser power of 100 mW. The CMX-4 laser pulse width is ca 1 μsec, and that for the Molectron nitrogen-pumped dye laser is ca 10 nsec. Use of the very short high-peak power Molectron laser pulse for resonance Raman scattering can be complicated by nonlinear optical processes that can compete with the Raman scattering process.[24] These pulsed laser sources also have significant pulse-to-pulse intensity fluctuations that require extensive signal averaging during the spectral scan. In principle, this can be alleviated by using a dual-channel electronic detection system that normalizes the Raman scattered intensity to the intensity of each of the incident laser pulses.[25] However, the dual-channel detection system cannot compensate for the intensity dependence of thermal lensing effects in the sample. Each laser pulse during a resonance Raman measurement results in sample absorption and temperature increases within the illuminated sample volume. The resulting sample density changes result in thermal lensing that defocuses the laser beam within the sample. Thus, the effective illuminated sample volume depends upon the incident laser pulse energy.

A fixed arrangement for the light collection optics results in variations

[24] L. D. Cheung, N.-T. Yu, and R. H. Felton, *Chem. Phys. Lett.* **55**, 527 (1978).
[25] S. A. Asher, Ph.D. Thesis, University of California, Berkeley, Report LBL-5375 (1976).

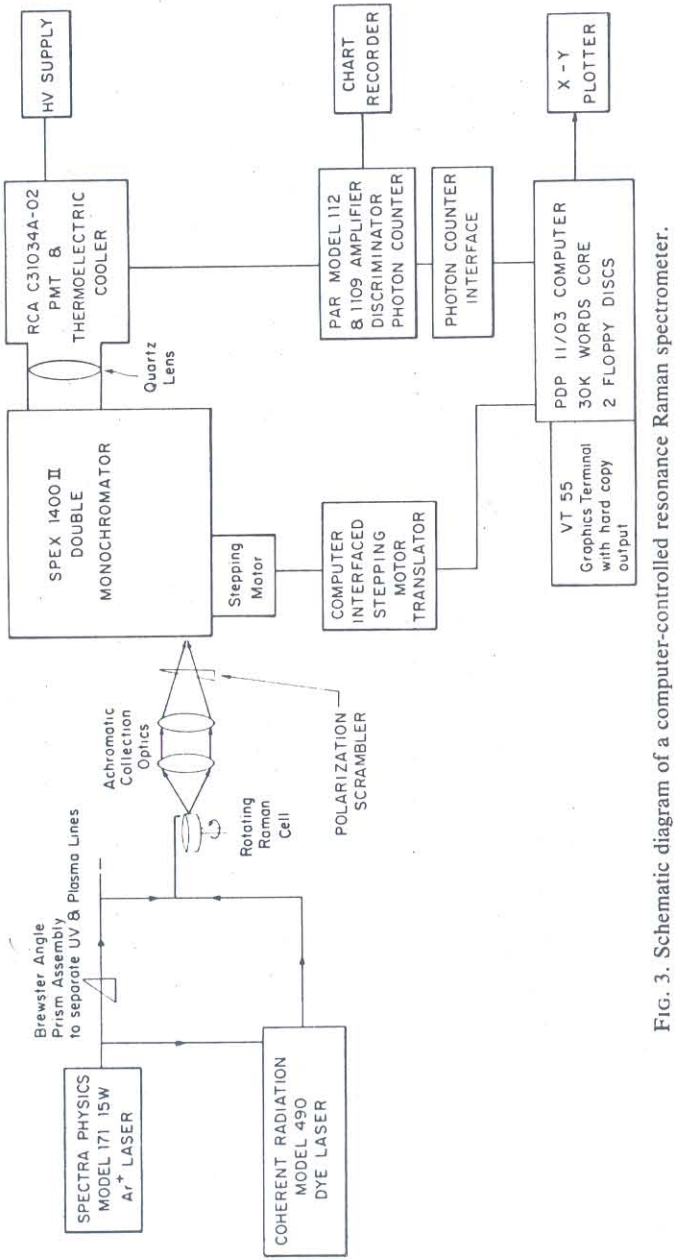

FIG. 3. Schematic diagram of a computer-controlled resonance Raman spectrometer.

for the light collection efficiency as the beam size changes. These variations depend nonlinearly on the incident pulse energy. The fluctuations in the light collection efficiency requires averaging of numerous laser pulses even with a dual channel system if typical photomultiplier detection is used. However, this problem is completely alleviated for vidicon and reticon detection systems, which examine large Raman spectral regions simultaneously; any light collection efficiency changes or pulse-to-pulse intensity fluctuations affect the entire spectrum simultaneously (see below).

A rotating or flowing Raman cell is generally used to avoid sample thermal decomposition in the laser beam. The rotating cell is generally made of quartz and can be used with <0.1 ml of sample. The centrifugal forces in the spinning cell (ca 1000 rpm) causes a thin film of the sample to layer on the cylindrical cell walls. The laser beam can be focused along this thin film, and the scattered light can be collected at 90° to the incident laser beam. Because the sample is quickly rotated through the beam, little sample heating occurs. A flow cell can also be used in which the sample recirculates through the laser beam.

The scattered light is collected and imaged into the entrance slit of a double monochromator. A polaroid analyzer can be used to measure the depolarization ratio of the Raman scattered peaks. A polarization scrambler, a wedge of birefringent quartz, is used to randomize the polarization of the collected light prior to its entrance into the monochromator. This avoids intensity artifacts that can occur due to the intrinsic polarization bias of monochromator gratings.

In Fig. 3 the scattered light intensity is detected by a photomultiplier with photon-counting detection electronics. A computer controls the monochromator scanning and accumulates data to allow signal averaging through repetitive scanning of the spectra.

Vidicon and Reticon detector arrays are clearly superior to the classical photomultiplier detection systems. They are essentially an array of light sensing devices. By removing the monochromator exit slit and using gratings with the appropriate dispersion, large regions of the Raman spectra can be simultaneously observed with significant increases in the system efficiency and signal-to-noise ratios.[26-31] As previously mentioned,

[26] Y. Talmi, *Anal. Chem.* **47,** 658 A (1975).
[27] W. H. Woodruff and S. Farquharson, *Anal. Chem.* **50,** 1389 (1978).
[28] R. B. Srivastava, M. W. Schuyler, L. R. Dosser, F. J. Purcell, and G. H. Atkinson, *Chem. Phys. Lett.* **56,** 595 (1978).
[29] J. Terner, C.-L. Hsieh, and A. R. Burns, and M. A. El-Sayed, *Proc. Natl. Acad. Sci. U.S.A.* **76,** 3046 (1979).
[30] R. Mathies and N.-T. Yu, *J. Raman Spectrosc.* **7,** 349 (1978).
[31] N.-T. Yu and R. B. Srivastava, *J. Raman Spectrosc.* **9,** 166 (1980).

the vidicon and Reticon arrays alleviate many of the problems intrinsic to pulsed excitation sources.

A number of recent instrumental advances have been utilized for heme protein resonance Raman studies. Shelnutt *et al.*[32,33] have devised a dual-chamber rotating Raman cell that is split down the middle to contain two different samples. The cell is rotated through the laser beam so that separate photon counting detection systems independently monitor each sample compartment as it rotates through the exciting beam. After accumulating separate datum for each sample the monochromator is scanned to an adjacent frequency until the two full spectra are accumulated. A difference spectrum is subsequently generated by subtracting the individual spectra. The advantage of this technique is that Raman shifts of <0.1 cm^{-1} can be reliably measured because both spectra are obtained essentially simultaneously; low frequency noise sources ($<$ sample rotation frequency) do not contribute to degradation of the signal-to-noise ratio of the difference spectrum. In addition, problems associated with frequency shifts between successively scanned spectra are prevented, since identical grating positions occur for each of the spectra.

Another recent technique that promises to yield important mechanistic data for hemoglobin cooperativity is kinetic Raman spectroscopy.[6-11a] In the case of carbon monoxyhemoglobin a pulsed laser source is used to photodissociate the CO ligand. The Raman spectra of the dissociated heme species is obtained with a second pulsed laser at some time subsequent to the photodissociation. The kinetic data indicate both fast and slow protein and heme alterations that are interpreted to result from movements of the iron from the heme plane, and tertiary, and quaternary protein conformational changes.[8,9,11,11a]

Sample Preparation

Resonance Raman heme protein measurements require sample volumes of ca 0.1 ml at micromolar to millimolar heme concentrations. The major requirement is an absence of fluorescent contaminants. In hemoglobin and myoglobin samples these may result from insufficient protein purification or protein thermal, chemical, or bacterial denaturation. Since the heme fluorescence is efficiently quenched by the iron, denatured protein fluorescence probably results from removal of the iron from the heme or a decomposition of the heme macrocycle.

Fluorescent contaminants can easily be removed by column chromatography on Sephadex CM-50 column resin.[34] Nagai *et al.* reported that isoelectric focusing on polyacrylamide gels is essential for resonance Raman measurements at low frequencies.[35] A rotating Raman cell is necessary to avoid thermal decomposition in the intense laser beam and, as Kitagawa and Nagai[36] have recently demonstrated, to avoid extensive heme photoreduction which can occur in methemoglobin derivatives upon excitation within the Soret band.

[32] J. A. Shelnutt, D. L. Rousseau, J. K. Dethmers, and E. Margoliash, *Proc. Natl. Acad. Sci. U.S.A.* **76,** 3865 (1979).

[33] J. A. Shelnutt, D. L. Rousseau, J. M. Friedman, and S. R. Simon, *Proc. Natl. Acad. Sci. U.S.A.* **76,** 4409 (1979).

Assignments and Structural Sensitivities of Heme Macrocycle Vibrations

Excitation within the α, β, and Soret bands of hemoglobin or model heme complexes results in enhancement of numerous Raman peaks between 100 and 1700 cm^{-1} whose relative intensities show a dramatic dependence upon the excitation wavelength as shown in Figs. 4A and B for Mn(III) etioporphyrin I (MnETP).[37] Figure 5 shows the corresponding absorption spectra of MnETP and indicates the excitation wavelengths used for obtaining the spectra in Fig. 4.

A combination of normal mode calculations and model heme resonance Raman studies using isotope substitution of the iron, the pyrrole nitrogens, and methine hydrogens as well as changing peripheral substituents have resulted in detailed assignments for many of the observed Raman peaks.[38-44] A number of the heme in-plane macrocyclic vibrational modes are sensitive to the electron density in the heme ring, to the spin state of the iron as it affects the distance between the center of the heme and the pyrrole nitrogens, and to the iron out-of-heme plane distance.

The extensive investigations of these vibrational modes by numerous groups have led to a variety of labeling schemes. This review adopts the convention initially used by Spiro and Burke.[44] Table I lists those resonance Raman peaks that have been characterized as monitors of heme structure.

[34] S. A. Asher and T. M. Schuster, *Biochemistry* **18,** 5377 (1979).

[35] K. Nagai, T. Kitagawa, and H. Morimoto, *J. Mol. Biol.* **136,** 271 (1980).

[36] T. Kitagawa and K. Nagai, *Nature (London)* **281,** 503 (1979).

[37] S. A. Asher and K. Sauer, *J. Chem. Phys.* **64,** 4115 (1976).

[38] T. Kitagawa, M. Abe, and H. Ogoshi, *J. Chem. Phys.* **64,** 4516 (1978).

[39] M. Abe, T. Kitagawa, and Y. Kyogoku, *J. Chem. Phys.* **64,** 4526 (1978).

[40] P. Stein, J. M. Burke, and T. G. Spiro, *J. Am. Chem. Soc.* **97,** 2304 (1975).

[41] T. Kitagawa, M. Abe, Y. Kyogoku, H. Ogoshi, H. Sugimoto, and Z. Yoshida, *Chem. Phys. Lett.* **48,** 55 (1977).

[42] T. Kitagawa, H. Ogoshi, E. Watanabe, and Z. Yoshida, *Chem. Phys. Lett.* **30,** 451 (1975).

[43] T. Kitagawa, M. Abe, Y. Kyogoku, H. Ogoshi, E. Watanabe, and Z. Yoshida, *J. Phys. Chem.* **80,** 1181 (1976).

[44] T. G. Spiro and J. M. Burke, *J. Am. Chem. Soc.* **98,** 5482 (1976).

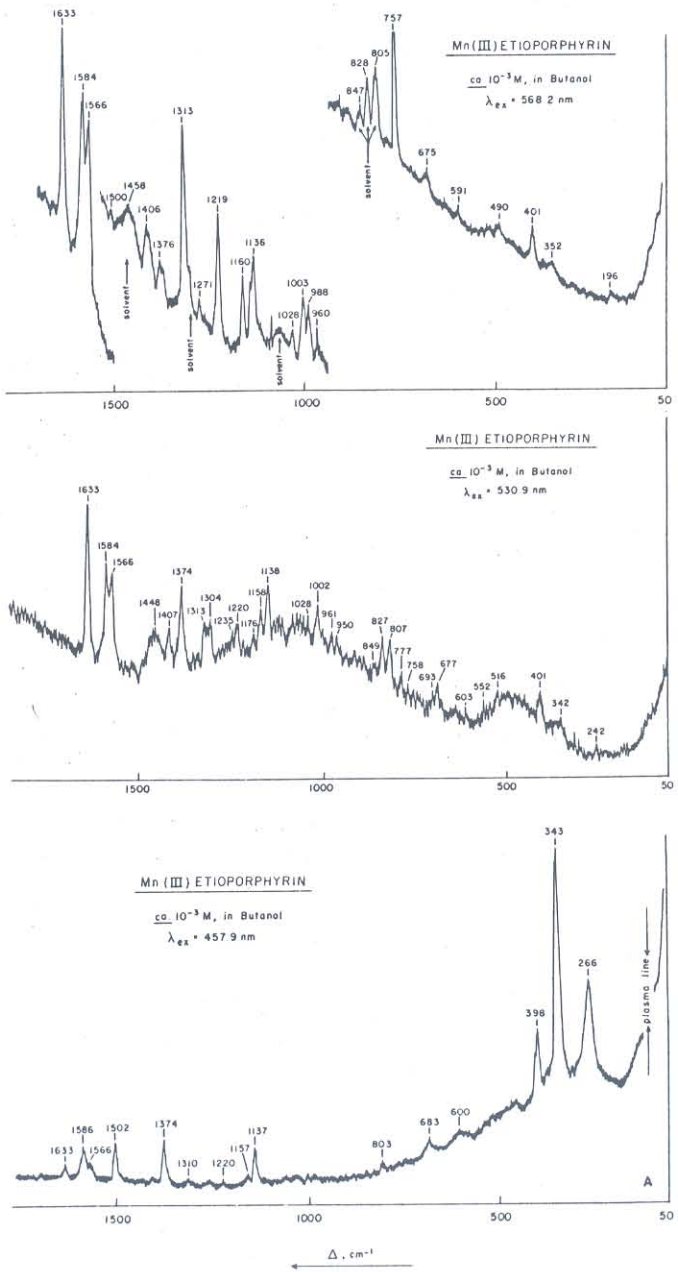

FIG. 4A.

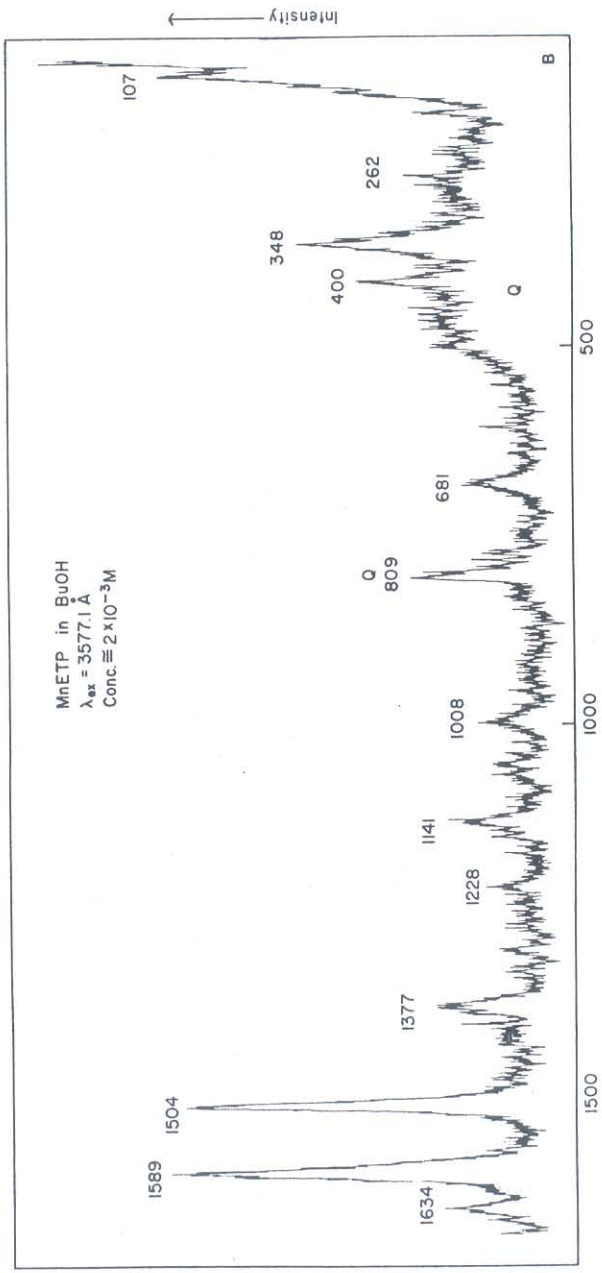

FIG. 4. Resonance Raman spectra of Mn(III) etioporphyrin I in butanol at different excitation wavelengths. The different excitation wavelengths result in distinctly different enhancement patterns. (A) Excitation in the visible spectral region. (B) Excitation in the UV. The positions of excitation within the Mn(III) etioporphyrin absorption spectrum are shown in Fig. 5. Bands I, II, IV, and V occur at 1374, 1502, 1586, and 1633 cm^{-1}, respectively. The frequency difference observed between spectra presumably are due to the interference of overlapping peaks whose contributions differs for different excitation wavelengths. (A) From Asher and Sauer[27]; (B) From Asher.[26]

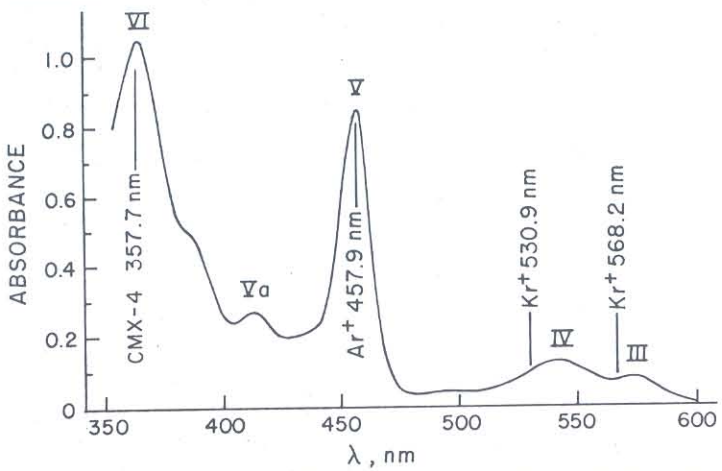

FIG. 5. Absorption spectrum of Mn(III) etioporphyrin I, 8.34×10^{-4} *M*, in butanol; path length, 1 cm. Also shown are the positions of the excitation wavelengths used to obtain the resonance Raman spectra in Fig. 4.

Heme Vibrations Sensitive to Electron Density

Band I occurs between 1360 and 1390 cm^{-1} and is strongly enhanced upon excitation within the Soret bands of heme proteins and model compounds.[45] This polarized Raman peak appears to be sensitive to the electron density in the heme ring and shifts to higher frequency upon oxidation of ferrous derivatives to ferric derivatives.[44-47] Some disagreement exists concerning the atomic displacement coordinates associated with the band I vibration. The normal coordinate analysis of Stein *et al.*[40] indicates a 38% contribution of C_α—C_β stretching, a 31% contribution of C_α—C_M stretching, and a 17% contribution of C_β—C_β stretching (the carbon labeling scheme is indicated in Fig. 6). In contrast, Abe *et al.*[39] calculate a 53% contribution of C_α—N (pyrrole) stretching and a 21% contribution of C_α—C_M bending. Meso carbon deuteration and ^{15}N isotope substitution studies in model heme compounds have been consistent with a large contribution from pyrrole nitrogen displacements.[38,48]

The heme electron density-frequency dependence of band I appears to result from the heme macrocycle bond order dependence on the electron

[45] T. G. Spiro and T. C. Strekas, *J. Am. Chem. Soc.* **96,** 338 (1974).
[46] H. Brunner, A. Mayer, and H. Sussner, *J. Mol. Biol.* **70,** 153 (1972).
[47] T. Yamamoto, G. Palmer, D. Gill, I. T. Sameen, and L. Rimai, *J. Biol. Chem.* **248,** 5211 (1973).
[48] J. M. Burke, J. R. Kincaid, S. Peters, R. R. Gagne, J. P. Collman, and T. G. Spiro, *J. Am. Chem. Soc.* **100,** 6083 (1978).

TABLE I
STRUCTURE-SENSITIVE HEME MACROCYCLIC VIBRATIONAL MODES[a]

Band	Frequency region	Polarization	Sensitivity	Enhancement[b]
I	1340–1390	p	Heme electron density	Soret
II	1470–1505	p	Heme core size	Soret
IV	1535–1575	ap	Heme core size	Visible, Soret
V	1605–1645	dp	Heme core size	Visible, Soret
VI[c]	1560–1600	p	Heme core size and peripheral substituents	Soret

[a] Data taken from references cited in text footnotes 43–45, 49, 52–56.
[b] Indicates spectral region in which resonance enhancement is observed for this mode.
[c] Callahan and Babcock.[56]

density contained within the lowest lying π^* antibonding orbital. The increased electron density in this orbital occurring for ferrous compared to ferric heme derivatives results in decreased heme macrocycle bond force constants and a shift of band I to lower frequency. For example, band I in high-spin deoxyHb^{II} shows a band I frequency of 1357 cm^{-1} whereas in both high-spin $Hb^{III}F$ and low-spin $Hb^{III}CN$ it occurs at 1373 cm^{-1}.[44,49]

The frequency of band I depends also upon the nature of the axial ligand. Those ligands that display π conjugation to the heme ring affect the band I frequencies through delocalization of charge through the heme ring, and the iron, and ligand orbitals[49] Spiro and Burke[44] noted a correlation in model heme compounds of band I as well as III and V frequencies to the π acid strengths of the axial ligands. They proposed that the frequencies of these bands decrease with increasing back-donation of elec-

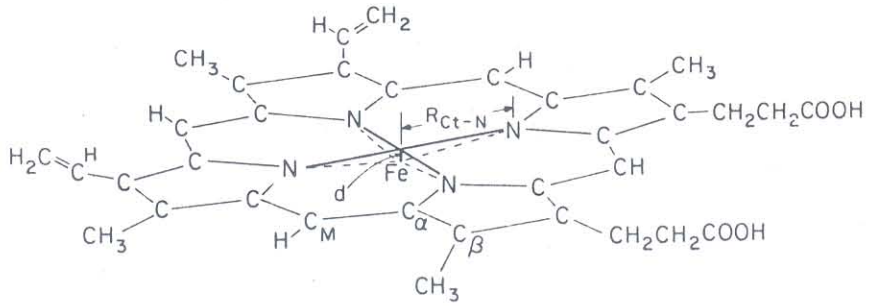

FIG. 6. Heme geometry and structure. The heme ring carbon atoms in the foreground are labeled. Also shown is the definition of the R_{Ct-N} distance and the distance of the iron from the heme plane, *d*.

[49] T. Kitagawa, Y. Kyogoku, T. Iizuka, and M. I. Saito, *J. Am. Chem. Soc.* **98,** 5169 (1976).

trons from the iron d_{xz} and d_{yz} orbitals to the π^* porphyrin orbitals. Strong π acid ligands compete for electrons and depopulate π^* porphyrin orbitals.

Because the frequency of band I depends on the electron density in the heme ring as influenced by the iron and its ligands, the frequency cannot be directly related to the formal charge on the iron. Thus, the $Hb^{II}O_2$ resonance Raman data[47] indicating a 1375 cm^{-1} band I frequency are not direct evidence for the Weiss model[50] of oxygen bonding. This model proposes that oxygen is bound as a superoxide ferric complex.[45]

Although the frequency of band I appears to depend mainly upon electron density in the heme macrocycle, it also shows an iron spin-state dependence for iron tetraphenylporphins.[48] In addition, a recent study of reconstituted myoglobins by Tsubaki *et al.*[51] indicates a dependence of band I frequencies on heme peripheral substituents. A 5 cm^{-1} frequency shift was observed between derivatives differing by formyl substitution of either the 2- or 4-vinyl group of the heme.

Heme Vibrations Sensitive to Heme Core Size

A number of heme macrocyclic modes occurring between 1470 and 1650 cm^{-1} appear to monitor the distance between the center of the heme and the pyrrole nitrogen atoms, R_{Ct-N} (Fig. 6). These bands can be identified by their frequency and polarization (Table I). Band II is a polarized Raman peak occurring between 1470 and 1505 cm^{-1} and is enhanced by excitation near the Soret absorption band. Band III, which is depolarized, occurs between 1535 and 1575 cm^{-1} overlapping band IV, which occurs between 1550 and 1590 cm^{-1}. However, because band IV is anomalously polarized ($\rho > 0.75$) it can be resolved by polarization measurements. Band V is depolarized and occurs between 1605 and 1645 cm^{1}. Bands IV and V are typically observed by excitation throughout the visible and near-UV spectral region and often dominate the resonance Raman spectra (Fig. 4).

It has been clear for some time[45] that the frequencies of all these vibrational modes depend upon the spin state of the iron and are little affected by the heme ring electron density. This is particularly true for band IV. Initially the iron spin-state frequency dependence of bands II, IV, and V was proposed to result from heme doming in the high-spin species, which resulted from out-of-heme plane iron displacements. The consequent decrease in heme π orbital conjugation was expected to result in decreased heme macrocycle bond force constants, which would lower the observed

[50] J. Weiss, *Nature (London)* **203,** 83 (1964).
[51] M. Tsubaki, K. Nagai, and T. Kitagawa, *Biochemistry* **19,** 379 (1980).

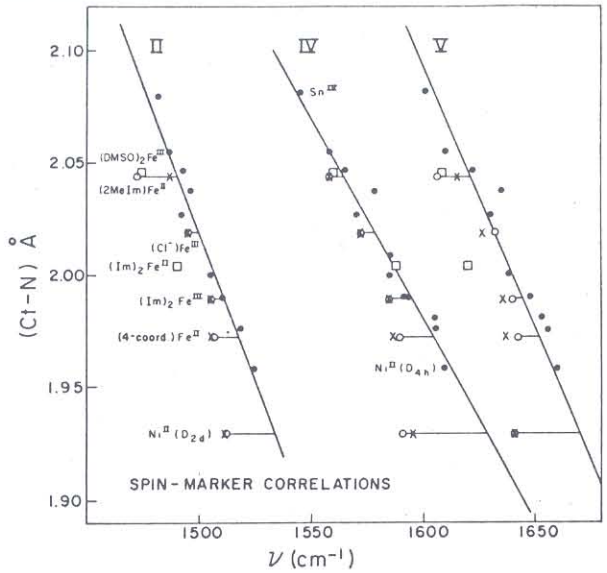

FIG. 7. Correlation between band II, IV, and V frequencies and the X-ray structural determination of the R_{Ct-N} distance in various heme model compounds. From Spiro *et al.*[55]

vibrational stretching frequencies. However, Spaulding *et al.*[52] in an extensive investigation of model heme compounds compared band IV resonance Raman frequencies to X-ray determinations of heme structure and discovered a direct linear correlation between the band IV frequency and the heme core size, R_{Ct-N} (Fig. 6). This study was extended by Huong and Pommier,[53] who proposed a linear relationship for bands IV and V of the form

$$\nu_i = K_i (A_i - R_{Ct-N}) \tag{7}$$

where ν_i is the frequency of the Raman peak and A_i and K_i are empirically determined constants for each of the Raman peaks. Additional work[54,55] indicates that a similar linear correlation exists for band II. The experimentally determined correlations between the bands II, IV, and V frequencies and the X-ray-determined R_{Ct-N} distances are shown in Fig. 7.[55]

Each of the vibrations that give rise to these bands contains significant

[52] L. D. Spaulding, C. C. Bhang, N.-T. Yu, and R. H. Felton, *J. Am. Chem. Soc.* **97,** 2517 (1975).
[53] P. V. Huong and J.-C. Pommier, *C. R. Acad. Sci. Paris, Ser. C* **285,** 519 (1977).
[54] A. Lanir, N.-T. Yu, and R. H. Felton, *Biochemistry* **18,** 1656 (1979).
[55] T. G. Spiro, J. D. Stong, and P. Stein, *J. Am. Chem. Soc.* **101,** 2648 (1979).

TABLE II
PARAMETERS RELATING RAMAN FREQUENCIES TO R_{Ct-N} DISTANCES[a]

Band	K_i (cm^{-1}/Å)	A_i (Å)	Comments
II[b]	375.5	6.01	Small dependence on π acid strength of axial ligand
IV[b]	555.6	4.86	
V[b]	423.7	5.87	Small dependence on π acid strength of axial ligand
VI[c]	300	7.30	Shows peripheral substituent frequency dependence

[a] The parameters A_i and K_i occur in the expression $\nu_i = K_i(A_i - R_{Ct-N})$. See text for details.
[b] From Spiro *et al.*[55]
[c] From Callahan and Babcock.[56]

contribution from methine bridge bond stretches as indicated by methine deuteration studies.[38,39,42,44,52] Apparently bands II, IV, and V correspond to vibrations ν_3, ν_{19}, ν_{10} of Abe *et al.*[39] with stretching contributions of 41% (C_α—C_m):31% (C_α—C_β), 67% (C_α—C_m):18% (C_α—C_β), and 49% (C_α—C_m):35% (C_α—C_β), respectively. The R_{Ct-N} frequency dependency appears to result from deformations involving a bending and stretching of the methine bridge bonds upon an R_{Ct-N} expansion. The resulting decreased π conjugation results in a decreased force constant for the C_α—C_M bonds leading to frequency decreases for bands II, IV, and V. The empirically determined parameters in Eq. (7) for bands II, IV, and V are tabulated in Table II. Also included are the parameters recently determined[56] for another heme vibration sensitive to the R_{Ct-N} distance occurring between 1560 and 1600 cm^{-1}, which is labeled band VI.

Band VI is a polarized peak observed with Soret band excitation. It can be resolved from the anomalously polarized band IV, which also occurs in the same spectral region by polarization measurements. Band VI presumably corresponds to the ν_2 mode calculated by Abe *et al.*[39] and primarily results from C_β—C_β stretching; as a result, this peak shows a twofold smaller R_{Ct-N} frequency dependence and a much larger peripheral substituent dependence than does band IV.

The heme structural sensitivity of bands II, IV, V, and VI can be utilized to study the dependence of heme geometry on ligand bonding and globin structure. Because of the predominant C_α—C_M stretching contribution to band II, IV, and V vibrations only small frequency shifts occur

[56] P. M. Callahan and G. T. Babcock, *Biochemistry* **20**, 952 (1981).

upon heme peripheral substituent changes, provided the methine carbons are protonated and the β carbons have carbon substituents.[55] For example, the empirical correlations between the R_{Ct-N} distance and the band IV frequency indicates a 0.002 Å/cm^{-1} frequency dependence. This represents a potential bond distance resolution surpassing X-ray or EXAFS measurements.

The R_{Ct-N} distance depends primarily on the effective radius of the iron atom and steric nonbonding interactions between the axial ligands and the pyrrole nitrogen orbitals. For example, in a comparison between the isolated α and β subunits of methemoglobin fluoride ($HB^{III}F$), Asher and Schuster[57] noted that the Fe—F stretching vibration in the α subunits occurred at 466 cm^{-1}, 5 cm^{-1} to lower frequency than that in the β subunits (471 cm^{-1}). An associated shift of ca 1.5 cm in the *opposite* direction to *higher* frequency was observed for band V (Fig. 8). These frequency shifts were interpreted to result from a larger displacement of the iron to the proximal heme side in the α subunits compared to the β subunits. The

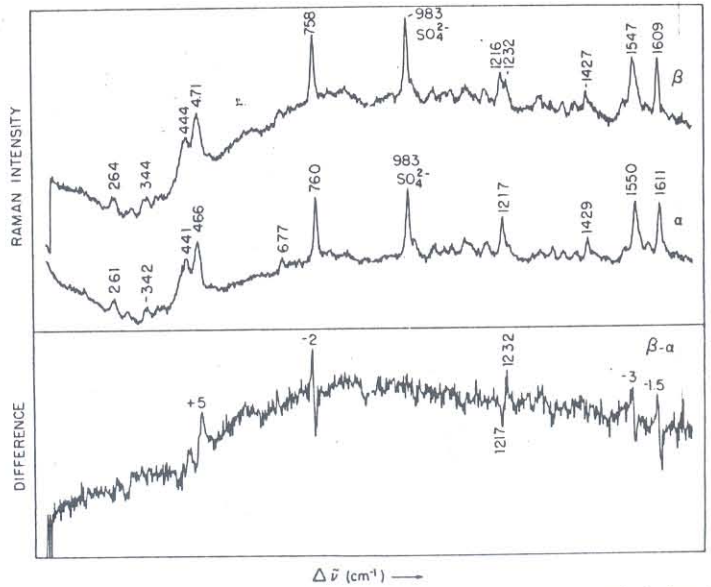

FIG. 8. Resonance Raman spectra of the fluoride derivatives of the ferric isolated α and β chains of hemoglobin and their Raman difference spectrum obtained by subtraction of the individual successively measured spectra. Note that small increases in the band IV and V frequencies occur in conjunction with a larger 5 cm^{-1} decrease in the Fe—F stretching frequency in the α subunits compared to the β subunits. From Asher and Schuster.[57]

[57] S. A. Asher and T. M. Schuster, *Biochemistry* **20**, 1866 (1981).

increased iron displacement results in an elongation of the α subunit Fe—F bond and lowered Fe—F stretching frequency. As the iron moves out of the heme plane, the heme core can contract leading to a decreased R_{Ct-N} distance and an increased band V frequency.

For identical spin states larger R_{Ct-N} distances with smaller band II, IV, and V stretching frequencies occur for ferrous hemes compared to ferric hemes. This results from an increased iron–pyrrole nitrogen bond length due to the decreased ferrous iron charge.[55] High-spin iron complexes show larger R_{Ct-N} distances and lowered bands II, IV–VI Raman frequencies than do low-spin complexes because of an increased electron density population of $d_{x^2-y^2}$ antibonding orbitals.[55] Six-coordinate complexes show a larger R_{Ct-N} distance than do 5-coordinate complexes because of the resulting ligand–pyrrole nitrogen repulsions, which tend to keep the iron centered in the heme plane; the iron in 5-coordinate complexes projects out of the heme plane toward the single axial ligand.

One important conclusion which has resulted from the heme protein and model compound resonance Raman studies of bands I–V is that no large perturbation of heme structure exists in hemoglobin and myoglobin compared to nonprotein bound hemes.[55] This important conclusion places constraints on any model for hemoglobin cooperativity and suggests that the chemistry involved should be consistent with that occurring in model iron porphyrins. However, Stong *et al.*[58] were able to interpret the bands I, II, IV, and V frequency shifts occurring upon conversion of $Hb^{III}NO$ from the R to the T conformation to indicate a cleavage of the α chain iron–proximal histidine bond, leaving the α chain irons 5-coordinate.

Although the frequencies of bands II, IV, and V depend primarily upon the R_{Ct-N} distance, bands II and V also show a secondary dependence upon the π acid strength of the axial ligands. It may be possible experimentally to uncouple effects of ligand π strength and R_{Ct-N} distance changes by comparing band II and V frequency shifts to that of band IV, which is almost insensitive to the nature of the axial ligand. A general frequency change for all these peaks would suggest a simple R_{Ct-N} distance change.

It has been suggested that each of these bands has a small frequency dependence upon the iron out-of-heme plane distance and upon heme doming.[55] However, this frequency dependence appears to be too small to use for a probe of either doming or the iron out-of-plane distance. Scholler and Hoffman estimate that a ca 2 cm^{-1} shift would occur for a 0.1 Å out-of-heme plane iron excursion in low-spin 6-coordinated hemes.[59]

[58] J. D. Stong, J. M. Burke, P. Daly, P. Wright, and T. G. Spiro *J. Am. Chem. Soc.* **102,** 5815 (1980).

[59] D. M. Scholler and B. M. Hoffman *J. Am. Chem. Soc.* **101,** 1655 (1979).

Iron–Axial Ligand Vibrations

Resonance Raman studies of vibrational modes involving the iron proximal histidine bond, as well as the bond between the iron and the sixth ligand, should directly monitor constraints imposed by the globin affecting bond strengths and ligand binding affinities. The vibrational frequencies of these modes should depend upon globin perturbations of the iron out-of-heme plane distance as well as upon interactions between these ligands and other species in the heme cavity.

Until recently it has been difficult to observe iron–axial ligand stretching vibrations due to the weak enhancements that occur upon 4500–6400 Å resonance Raman excitation. Enhancement of iron–axial ligand vibrational modes does not generally occur with excitation within $\pi \rightarrow \pi^*$ electronic transitions because iron–ligand vibrations appear to be uncoupled from the resonant α, β, and Soret electronic transitions. However, excitation within charge transfer bands often results in enhancement of iron–axial ligand vibrational modes and, on occasion, internal vibrations occurring within the ligands.

Iron–Sixth Ligand Vibrations

A number of charge transfer absorbtion bands have been assigned in heme complexes. The first example is an in-plane charge transfer transition between the heme π orbitals and the d_{xz}, d_{xz} orbitals of the iron.[25,34,60,61] These electronic transitions occur in $Hb^{III}F$, $Mb^{III}F$ and in the high-spin species of $Hb^{III}OH$ and $Mb^{III}OH$.[60,61] Excitation within these ca 6000 Å absorption bands enhances Fe—F and Fe—O stretching vibrations.[25,34,57,62,63]

Enhancement of iron–ligand stretching vibrations are also observed for excitation in *z*-polarized charge transfer bands. These charge transfer electronic transitions occur either between porphyrin π orbitals and the iron d_{z^2} orbital, or between the iron orbitals and the ligand orbitals; Fe—N_3 stretching vibrations at 413 cm^{-1} have been observed with excitation with the *z*-polarized charge transfer transition of $Hb^{III}N_3$ at ca 6400 Å.[62] A number of iron–axial ligand vibrational modes have been ob-

[60] H. Kobayashi, Y. Yanagava, H. Osada, S. Minami, and M. Shimizu, *Bull. Chem. Soc. Jpn.* **46,** 1471 (1973).

[61] A. Churg, H. A. Glick, J. A. Zelano, and M. W. Makinen, *in* "Biological and Clinical Aspects of Oxygen" (W. S. Caughey, ed.), p. 125. Academic Press, New York, 1980.

[62] S. A. Asher, L. E. Vickery, T. M. Schuster, and K. Sauer, *Biochemistry* **16,** 5849 (1977).

[63] S. A. Asher and T. M. Schuster, *In* "Interactions between Iron and Proteins in Oxygen and Electron Transport" (C. Ho., W. A. Eaton, J. P. Collman, Q. H. Gibson, J. S. Leigh, Jr., E. Margoliash, J. K. Moffat, and W. R. Scheidt, eds.). Elsevier, Amsterdam, 1981, in press.

served upon excitation within ligand–iron charge transfer transitions. The most important example is the Fe—O stretch enhanced by excitation at 4880 Å in $Hb^{II}O_2$ and $Mb^{II}O_2$ as observed by Brunner.[64] The enhancement of the Fe—O stretching vibration presumably results from the *z* polarized charge transfer transition observed in single crystal absorption studies which was assigned to a $d \rightarrow d$ electronic transition that vibronically borrows intensity from an intense iron to oxygen ligand UV charge transfer transition.[65] A similar enhancement is observed for the Fe—N stretching vibration in $Hb^{II}NO$ and $Mb^{II}NO$.[58,66]

Spiro and Burke[44] and Wright *et al.*[67] have observed enhancement of the Fe—N(pyridine) stretching vibrations within the iron→pyridine charge transfer transitions of bispyridine Fe^{2+}-mesoporphyrin I-dimethyl ester. More important, they also observed large enhancements for internal pyridine vibrations indicating that internal axial ligand vibrations could be observed upon excitation within certain charge transfer absorption bands.

The enhancement of the Fe—N(azide) stretch at 413 cm^{-1} observed by Asher *et al.*[62] in $Hb^{III}N_3$ with excitation at 6383 Å was suggested to result from a *z*-polarized charge transfer transition occurring in the high-spin azide species (Fig. 9); $Hb^{III}N_3$ exists in a thermal spin-state equilibrium containing 10% high- and 90% low-spin iron species. However, subsequent studies have questioned this assignment and have presented some important new data on the possible existence of novel charge transfer transitions and new axial ligand resonance Raman enhancement mechanisms.

Desbois *et al.*[68] exciting within the Soret absorption band observed enhancement of a ca 570 cm^{-1} peak, which they assigned to the Fe—N(azide) stretch because it shifted by 16 cm^{-1} upon ^{15}N azide isotope substitution. However, Tsubaki *et al.*[69] also exciting within the Soret band found that the 570 cm^{-1} peak was depolarized and assigned it to an internal azide stretching vibration. They also observed enhancement of a number of other internal azide stretching vibrations and suggested that the Soret band resonance Raman enhancement observed[68] for numerous high-spin Hb^{III} derivatives results from the existence of charge transfer transitions underlying the $\pi \rightarrow \pi^*$ Soret absorption band.

[64] H. Brunner, *Naturwissenschaften* **61,** 129 (1974).
[65] W. A. Eaton, L. K. Hanson, P. J. Stephens, J. C. Sutherland, and J. B. R. Dunn, *J. Am. Chem. Soc.* **100,** 4991 (1978).
[66] G. Chottard and D. Mansuy, *Biochem. Biophys. Res. Commun.* **77,** 1333 (1977).
[67] P. G. Wright, P. Stein, J. M. Burke, and T. G. Spiro *J. Am. Chem. Soc.* **101,** 3531 (1979).
[68] A. Desbois, M. Lutz, and R. Banerjee, *Biochemistry* **18,** 1510 (1979).
[69] M. Tsubaki, R. B. Srivastava, and N.-T. Yu, *Biochemistry* **20,** 946 (1981).

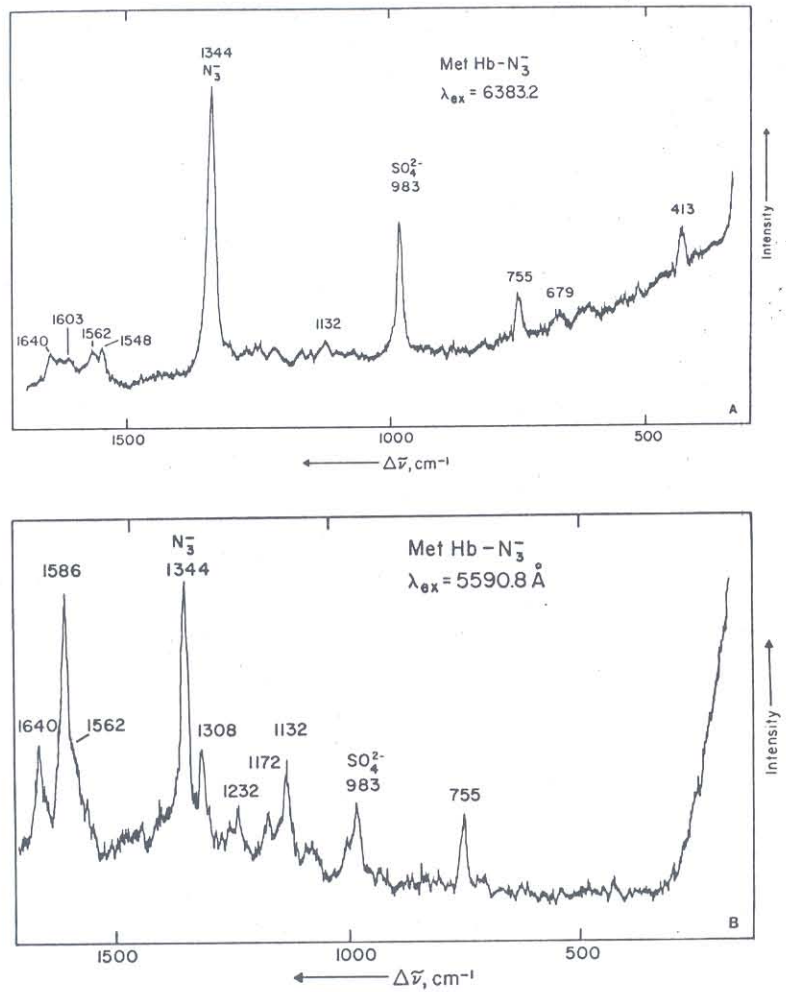

FIG. 9. Resonance Raman spectra of $Hb^{III}N_3$. (A) Excitation at 6383 Å in a *z*-polarized charge transfer transition. The Fe—N_3^- stretch is enhanced at 413 cm^{-1} as are vibrations from both the low- and high-spin species. $Hb^{III}N_3$ exists in thermal spin-state equilibrium at room temperature. Separate band V peaks are clearly resolved for each of the spin-state species. The 1640 cm^{-1} and 1603 cm^{-1} peaks correspond to band V from the low-spin and high-spin species, respectively. (B) Excitation at 5590.8 Å enhances only the low-spin-state Raman peaks. Bands IV and V occur at 1586 and 1640 cm^{-1}, respectively. The 983 cm^{-1} peak results from Na_2SO_4 added to the sample as an internal standard, and the 1344 cm^{-1} peak results from uncomplexed azide added to the sample in excess. From Asher *et al.*[62]

Tsubaki *et al.*[69] also observed the enhancement of the 413 cm^{-1} peak with ca 6400 Å excitation, as did Asher *et al.*[62] By ^{15}N isotope substitution Tsubaki *et al.* were able to confirm the assignment[62] of this peak to the Fe—N(azide) stretching vibration. However, from a temperature-dependent resonance Raman study they found that as the temperature was decreased the intensity of the 413 cm^{-1} peak *increased* in parallel with the increased intensity of low-spin bands IV and V peaks between 1500 and 1650 cm^{-1}. Because of the low-spin ground state expected for the thermal spin-state equilibrium they interpreted these data to indicate that the 413 cm^{-1} peak resulted from a low-spin state $Hb^{III}N_3^-$ species rather than the high-spin state species assigned by Asher *et al.*[62]

Although the data suggest an assignment of the Fe—N stretch at 413 cm^{-1} to the low-spin $Mb^{III}N_3^-$ species because of the empirical correlation between the intensities of the low-spin band IV and V peaks and that of the 413 cm^{-1} peak, they are not sufficient for an unequivocal and conclusive assignment. It is possible that the excitation profiles for the 413 cm^{-1} and the band IV and V peaks have a temperature dependence such that the intensities of these bands fortuitously increase together as the temperature decreases. Using changes in resonance Raman intensities to unequivocally assign spin-state species requires a determination of the temperature dependence of the excitation profiles of each of the peaks. This is especially important in charge transfer absorption bands

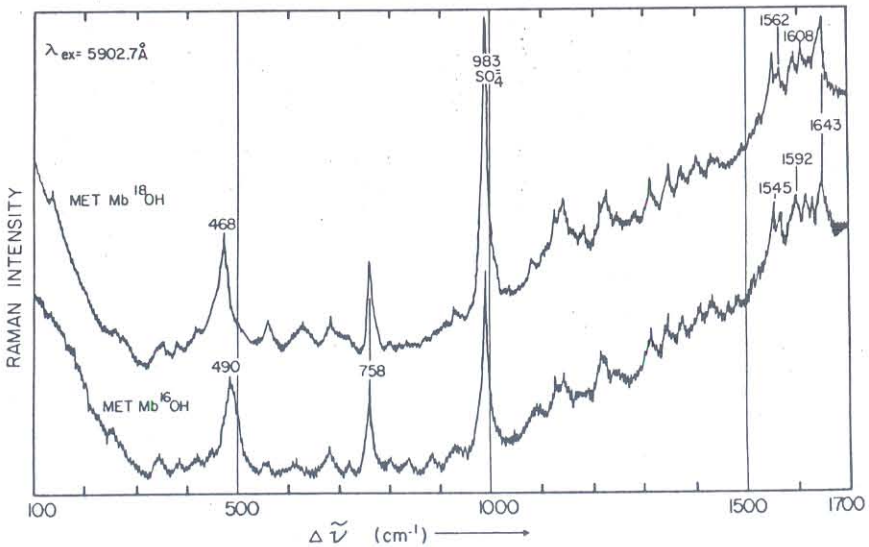

FIG. 10. Resonance Raman spectra of $Mb^{III16}OH$ and $Mb^{III18}OH$. The 22 cm^{-1} isotope frequency shift confirms the assignment of the 490 cm^{-1} peak to an Fe—O stretch. The high- and low-spin band V peaks occur at 1608 and 1644 cm^{-1}, respectively. From Asher and Schuster.[34]

because these absorption bands often display large line width and λ_{max} temperature dependencies.[26] A conclusive assignment for the species giving rise to the 413 cm^{-1} peak could more easily be obtained from a low temperature (~ 10°K) resonance Raman measurement of $Mb^{III}N_3^-$. At these temperatures only the low-spin species is present. If the 413 cm^{-1} were present, this would conclusively assign this peak to the low-spin species.

Excitation profile measurements can be used to resolve absorption spectra of thermal-spin state mixtures into contributions from the individual spin-state species. Asher and Schuster[57] assigned the 490 cm^{-1} Raman peak of $Mb^{III}OH$ (Fig. 10) to the Fe—O stretch in the high-spin iron species by correlating the excitation profile maxima of the Fe—O stretch to that of the high-spin band IV and V peaks. The 490 cm^{-1} $Mb^{III}OH$ Fe—O stretch has an excitation profile maximum at 6000, close to that of the 1608 cm^{-1} high-spin band V peak. The 1644 cm^{-1} low-spin band V peak shows its excitation profile maximum at ca 5800 Å (Fig. 11). This effect

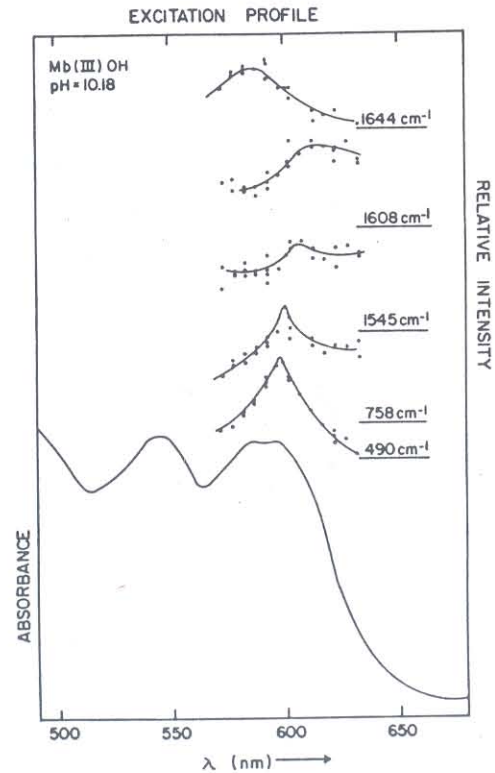

FIG. 11. Excitation profile and absorption spectrum of $Mb^{III}OH$. From Asher and Schuster.[34]

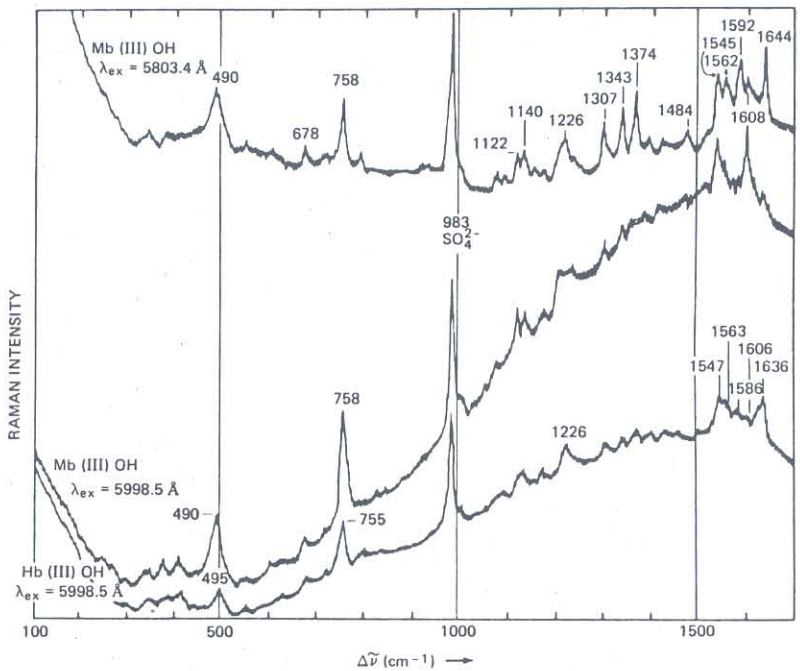

FIG. 12. Resonance Raman spectra of $Mb^{III}OH$ excited at 5803.4 Å and 5998.5 Å and $Hb^{III}OH$ excited at 5998.5 Å. Bands IV and V of $Mb^{III}OH$ occur at 1562 and 1608, and 1592 and 1644 cm^{-1} for the high- and low-spin species, respectively. The low-spin 1592 and 1644 cm^{-1} peaks are very intense with 5800 Å excitation, and the 1562 and 1608 high-spin peaks as well as the 490 cm^{-1} Fe—O stretch show maximum enhancement with 6000 Å excitation. From Asher and Schuster.[34]

can be clearly observed in the individual resonance Raman spectra of $Mb^{III}OH$ excited at 5800 Å and 6000 Å (Fig. 12). The resonance Raman spectra of $Hb^{III}OH$ with excitation at 6000 Å is also shown in Fig. 12.

The enhancement observed for iron–ligand vibrational modes depends upon the nature of the resonant charge transfer electronic transition. Enhancement of the internal azide stretching vibrations as well as the iron–azide stretching vibration upon Soret band excitation presumably results from a metal–azide charge transfer electronic transition involving internal azide bonding orbitals.[68,69] In contrast, the 6400–6500 Å charge transfer band iron–azide stretch enhancement probably results from an azide–metal charge-transfer transition involving only nonbonding azide orbitals[62,69]; enhancement of internal azide stretching vibrations is not observed.

The observation of iron–axial ligand vibrational enhancement for excitation within the Soret band of numerous high-spin Met derivatives and

MbO_2 suggests the existence of charge transfer transitions. Although there are *no* symmetry reasons preventing enhancement of out-of-plane axial ligand vibrations in formally C_{4v} symmetry hemes, if the Soret absorption band involves pure porphyrin macrocyclic orbitals uncoupled from the metal, it is difficult to rationalize iron–axial ligand enhancement, particularly enhancement of internal ligand vibrations. However, any differential mixing of metal, ligand, and porphyrin π orbital between the ground and excited states results in some charge transfer character for the heme electronic transition.

A new type of charge transfer transition has been observed in reconstituted azide Mn^{3+}-myoglobin.[70] This charge transfer transition occurring between 4000 and 4600 Å shows enhancement of heme macrocyclic vibrational modes and internal azide stretching vibrations. However, because no enhancement was observed for the Fe—N (azide) stretch, this absorption band was assigned to an azide (π) → porphyrin (π^*) charge transfer transition.[70]

Iron–Proximal Histidine Stretching Vibration

The most elusive iron–axial ligand stretching vibration has been that involving the iron–proximal histidine bond (Fe—N_ϵ). Because this bond represents the only covalent linkage between the heme and the globin, it represents a primary pathway for protein control of ligand affinity. The difficulty in assigning the Fe—N_ϵ stretching vibration results from the weak intensity enhancement occurring for this vibration and problems associated with preparing appropriate model compounds to perform isotope substitution studies in order to confirm the assignment of the vibration.

Initial assignments of the Fe—N_ϵ stretch to either a 411 cm^{-1} Raman peak[68] or 380 cm^{-1} Raman peak[71] have not been supported by more recent data.[35,72–75] Kitagawa *et al.*[73] and Nagai *et al.*[35] have presented strong evidence from $^{54}Fe \rightarrow {}^{56}Fe$ isotope substitution studies and model compound studies[35,75] that a ca 220 cm^{-1} peak in deoxyHb has a significant contribution from stretching of the Fe—N_ϵ bond. This 200–225 cm^{-1} Raman peak shows the largest frequency difference between the R and T protein conformations[35,74] of deoxyHb of any peak in the resonance Raman spectrum. This 220 cm^{-1} Raman peak is observed only with excitation within the Soret band of deoxyHb or deoxyMb at 4579 or 4416 Å. The corre-

[70] N.-T. Yu and M. Tsubaki, *Biochemistry* **19,** 4647 (1980).
[71] J. Kincaid, P. Stein, and T. G. Spiro, *Proc. Natl. Acad. Sci. U.S.A.* **76,** 549 (1979).
[72] J. Kincaid, P. Stein, and T. G. Spiro, *Proc. Natl. Acad. Sci. U.S.A.* **76,** 4156 (1979).
[73] T. Kitagawa, K. Nagai, and M. Tsubaki, *FEBS Lett.* **104,** 376 (1979).
[74] K. Nagai and T. Kitagawa, *Proc. Natl. Acad. Sci. U.S.A.* **77,** 2033 (1980).
[75] H. Hori and T. Kitagawa, *J. Am. Chem. Soc.* **102,** 3608 (1980).

sponding Fe—N_ϵ stretches in other heme derivatives have not yet clearly been identified.

Dependence of Axial Ligand Vibrations on Globin Structure

Studies of the Fe—N_ϵ stretch as well as the iron–sixth ligand stretches has resulted in a number of surprising results relevant to the hemoglobin cooperativity mechanism. For example, in an incisive study of the frequency dependence of the Fe—O stretching vibration upon globin quaternary structure Nagai *et al.*[35] found no systematic difference in the Fe—O stretching frequency between the R and T quaternary structure. On the other hand, in studies of the Fe—N_ϵ stretch in NES des-Arg-α141-Hb and deoxy des-His-β146-Arg-α141-Hb they observed a 4 cm^{-1} shift to lower frequency upon conversion of the protein from the R to T quaternary form (Fig. 13). Although these data lend qualitative support for a proximal histidine–iron bond strain model for hemoglobin cooperativity, the strain energies estimated to be associated with these small frequency shifts are about two orders of magnitude smaller than the free energy of cooperativity.

Larger Fe—N_ϵ frequency shifts have been observed for valency hybrids of hemoglobin in the R and T conformations.[74] The Fe—N_ϵ vibrational frequencies in the R conformation of deoxyHb were identical to those observed for the isolated deoxy chains. However, upon conversion of valency hybrids from the R to T form with either the α or β chains oxidized to the Met form, Kitagawa and Nagai[74] observed a 15 cm^{-1} shift for the Fe—N_ϵ stretch in the deoxy α chains compared to a 4 cm^{-1} shift for the deoxy β chains. A similar α subunit selective Fe—N_ϵ frequency decrease was observed when comparing T state deoxyHb Milwaukee (oxidized β chains) to deoxyHb Boston (oxidized α chains). These data indicate a selective decrease in the T state for the α chain Fe—N_ϵ force constant and an estimated stored strain energy that is eight times larger for the α chains than for the β chains.[74] However, the estimated strain energies still represent only a small fraction of the free energy of cooperativity.

Another study that has been informative about the relationship between the iron–ligand force constant and the ligand binding affinity is the examination of the frequency dependence of the Fe—O bond in reconstituted oxymyoglobins when the heme peripheral vinyl groups are substituted by formyl groups. Comparing the four possibilities, the native 2-vinyl-4-vinyl, 2-formyl-2-vinyl, 2-vinyl-4-formyl, 2-formyl-4-formyl, it was found that the oxygen affinities of these derivative differed by a factor of 5, but the Fe—O stretching frequency was identical within ± 1 cm^{-1}, indicating that for these derivatives there is no observable relationship between ligand affinity and iron–ligand force constant. Interestingly, IR studies of the corresponding carbon monoxy derivatives indicate 10 cm^{-1} frequency differences for the internal C=O, carbon monoxy stretching vibrations. The lowest frequency occurs for the derivative with the lowest oxygen affinity. Unfortunately, the Fe—CO vibration was not observed in the resonance Raman spectra of the carbon monoxy derivatives, nor was the O=O stretch monitored in the oxy derivatives.

Studies of the dependence of the Fe—O stretching frequency upon the heme oxygen affinity have been reported for the 1-methyl-, 1,2-dimethyl-, and 2-methylimidazole oxy and deoxy complexes of "picket-fence por-

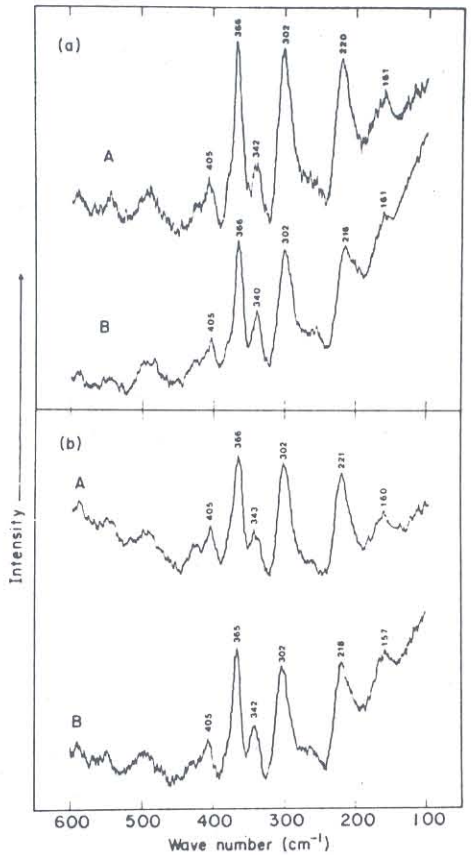

FIG. 13. Effect of R to T transition on the ca 220 cm^{-1} Fe—N_ϵ stretching vibration in deoxy NES des-Arg-α141-Hb (a) and deoxy-des-His-146–Arg α141-Hb (b). Trace A; R state, without inositol hexaphosphate (IHP); trace B; T state, 2 m*M* IHP. Laser excitation wavelength, 4579 Å. From Nagai *et al.*[35]

phyrin."[75,76] Hori and Kitagawa[75] examined the Fe—O stretching frequency in 1-methyl- and 1,2-dimethyl oxy picket-fence porphyrin derivatives, as did Walters *et al.*[76] However, in contrast to Walters *et al.*, Hori and Kitagawa found no Fe—O stretching frequency difference between these derivatives in CH_2Cl_2 solution, whereas Walters *et al.* found a 4 cm^{-1} decrease for the 1,2-dimethylimidazole derivative compared to the 1-methylimidazole derivative. Both groups found that the Fe—O vibration occurred at a lower frequency in crystals. However, Hori and Kitagawa found that the 1-methyl and 1,2-dimethyl derivatives had identical 555 cm^{-1} Fe—O stretching frequencies, whereas Walters *et al.* found that the Fe—O stretch in crystals of the 1-methyl, 2-methyl, and 1,2-dimethyl derivatives occur at 567, 557, and 558 cm^{-1}, respectively. Walters *et al.*[76] pointed out that single-crystal X-ray diffraction studies indicate that steric interactions between the bulky 2-methyl group and the heme ring pulls the iron from the heme plane toward the imidazole ligand, which results in elongations of both the Fe—O and Fe—N (imidazole) bonds. Indeed, Hori and Kitagawa found evidence for Fe—N (imidazole) bond elongation in the deoxy picket-fence porphyrin derivatives dissolved in CH_2Cl_2. They found a decreased Fe—N (imidazole) frequency in both 2-methylimidazole (209 cm^{-1}) and 1,2-dimethylimidazole (200 cm^{-1}) compared to the 1-methylimidazole (225 cm^{-1}) derivative of deoxy picket-fence porphyrin. Some of the apparent disagreement between these two groups may result from the breadth and weak intensities that occur for the Fe —O and Fe—N (imidazole) stretching vibration. However, the 10 cm^{-1} Fe—O frequency shift observed in the crystals correlates with a difference of three orders of magnitude between the oxygen affinities of the 1-methyl- and 2-methylimidazole complexes. These data suggest that the frequency of the Fe—O stretch is a poor monitor of ligand affinity and/or may suggest that the oxygen binding free-energy differences between these derivatives is not localized in the Fe—O bond.

Isotope substitution studies indicate that the iron–axial ligand stretches are uncoupled from other heme vibrations; the frequency shifts observed are essentially identical to those expected from a mass change in a pure diatomic vibration. For example, the 22 cm (± 2 cm^{-1}) frequency shift observed between $Mb^{III}{}^{18}OH$ and $Mb^{III}{}^{16}OH$ (Fig. 10) is exactly that expected from a harmonic oscillator approximation.[34,62] Similar behaviors are observed for the FeO_2, FeNO, and FeN_3 stretching vibrations in $Hb^{II}O_2$, $Hb^{II}NO$, and $Fe^{III}N_3^-$.[64,66–69]

Because the iron–axial ligand vibrational modes are essentially diatomic stretches uncoupled from other heme vibrations, the observed frequency shifts are direct measures of force constant changes. Unfortunately, it is difficult reliably to assign the frequency shifts to bond length changes or strain energy differences. For covalently bound ligands, Badger's rule as modified by Herschbach and Laurie[77] has been used to relate the calculated force constants to the iron–ligand bond lengths.[71]

$$r = d_{ij} + (a_{ij} - d_{ij})\, k^{-1/3} \tag{8}$$

where r is the bond length, d_{ij} and a_{ij} are empirically determined parameters for the atoms involved, and k is the vibrational stretching force constant. This relationship was empirically derived for diatomic molecules, and its validity for polyatomic ones has not been adequately tested. Indeed, a recent study by Walters *et al.*[76] demonstrated that the use of Badger's rule to calculate the Fe—O bond elongation from the measured Fe—O frequency shift between 1-methyl- and 2-methylimidazole picket-fence porphyrin complexes in crystals leads to a 15-fold underestimate for the Fe—O bond elongation when compared to the X-ray diffraction measurements.[76] One problem associated with the use of Badger's rule or other similar models, such as Morse potentials[35] as well as electrostatic models,[34] is that it is difficult to treat the important repulsive interactions between the heme pyrrole nitrogen orbitals and the axial ligand orbitals. Further, the use of vibrational frequencies as measures of bond strengths and energies rests on the assumption of a correlation between the vibrational force constant and the bond energy. The force constant is the second derivative of the potential, evaluated at the minimum of the diatomic molecular potential well, at the equilibrium bond length. The force constant-bond energy correlation is only valid to the extent that the magnitude of this second derivative measures the potential well depth.

An electrostatic model was used by Asher and Schuster[34] to treat the bond length dependence of iron–axial ligand stretching frequencies in the ionically bound ligands occurring in the high-spin fluoride, hydroxide, and azide methemoglobin and metmyoglobin derivatives. In the case of the hydroxide derivatives shown in Fig. 12 the 5 cm^{-1} shift in the Fe—O stretching frequency between $Hb^{III}OH$ (495 cm^{-1}) and $Mb^{III}OH$ (490 cm^{-1}) was estimated to result from a 0.01 Å increase in the $Mb^{III}OH$ Fe—O bond length. Similar ca 0.01 Å elongations were estimated to occur for the Fe—F bonds for $Mb^{III}F$ compared to the isolated $\alpha^{III}F$ subunits, and for the isolated $\alpha^{III}F$ subunits compared to the isolated $\beta^{III}F$ subunits.[57]

Hookes spring models can be used to estimate bond strain energies if the bond length changes and the equilibrium unstrained diatomic bond

[76] M. A. Walters, T. G. Spiro, K. S. Suslick, and J. P. Collman, *J. Am. Chem. Soc.* **102**, 6857 (1980).

[77] D. R. Herschbach and V. W. Laurie, *J. Chem. Phys.* **35**, 458 (1961).

lengths are known, and if the force constant is known as a function of bond length. Because each of these parameters can be only crudely estimated at present, and strain energy estimates should be considered very rough. However, the energies calculated using these crude models are reasonable and suggest that significantly less than the 3.6 kcal/mol heme strain energy is stored in the Fe—O or Fe—N_ϵ bonds.[35,59,71,74] The strain energy difference in the Fe—F bonds between $Hb^{III}F$ and $Mb^{III}F$ was estimated by Asher and Schuster using an electrostatic model[34,37] to be ca 1 kcal/mol. This value was very close to the experimentally observed difference in the fluoride binding enthalpy.

Models using Badger's rule, Morse potentials, and electrostatics to correlate Raman frequency shifts to bond length changes and strain energies contain gross approximations, and the results can be considered to be only rough estimates. However, work has begun on more sophisticated and realistic models to include effects such as repulsive interactions between the ligands and the pyrrole nitrogens as well as heme doming effects.[3,78]

Raman Evidence for Noncovalent Heme–Globin Interactions

The Raman differences technique (RDS) pioneered by Shelnutt *et al.*[32,33] permits reliable detection of extremely small frequency shifts (<0.1 cm^{-1}) between different hemoglobin derivatives. Shelnutt *et al.*[33] observed experimentally a correlation between the frequency of band I, the heme electron density-sensitive heme macrocyclic vibration, and the quaternary structure of a series of chemically modified deoxyhemoglobins. These derivatives occur in protein conformations that display the normal stability and ligand affinity of the deoxy (T) quaternary structure, and the high-ligand affinity structures in which the T deoxy quaternary structure does not occur and where the protein is considered to exist in the R quaternary form (Fig. 14). These data indicate a continuous frequency decrease for all the Raman modes examined as the high ligand affinity R protein quaternary form is stabilized (Fig. 14). Shelnutt *et al.* drew special attention to the band I frequency decrease (1.3 ± 0.1 cm^{-1}) between human deoxyHb A in the T quaternary structure and NES des-Arg-Hb A in the R form. Comparing these data with previous results[32] from an extensive study of cytochrome *c* proteins from different species, which indicated that similar RDS band I shifts were correlated with interactions between aromatic amino acids and the heme, Shelnutt *et al.* conjectured that the band I RDS frequency shift between the R and T forms

[78] A. Warshel and R. M. Weiss, *J. Am. Chem. Soc.* **103**, 446 (1981).

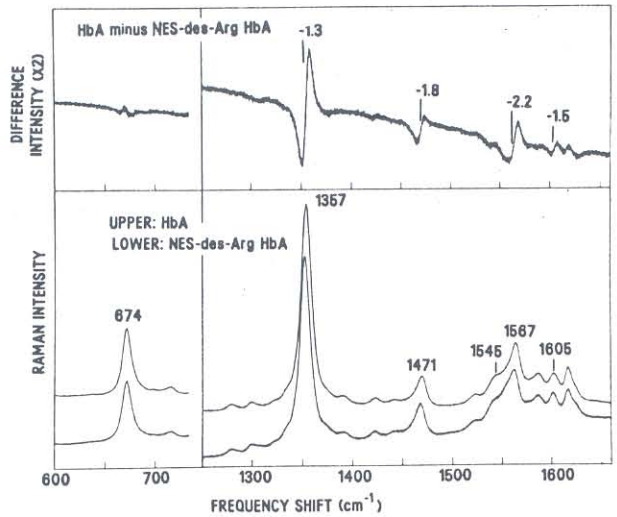

FIG. 14. Resonance Raman spectra (lower) and Raman difference spectra obtained using the RDS technique (upper) of deoxyHb A (T state) and NES des-Arg-α141-Hb A (R state). Laser excitation, 4579 Å. The frequency shifts are labeled above the difference spectrum. From Shelnutt *et al.*[33]

of deoxyHb resulted from changes in intermolecular interactions between the heme and aromatic amino acid side chains, such as phenylalanine CDI or G5 of the globin. This novel mechanism proposes that a differential charge transfer occurs between the heme and aromatic amino acid rings to populate the π^* heme orbitals to a greater extent in the R quaternary form than in the T quaternary form. This model proposes that the resulting charge-transfer stabilization energy could account for a significant portion of the free energy of cooperativity. Interestingly, a further RDS study[79] of methemoglobin derivatives in the R and T forms indicated that band I shifts in precisely the opposite direction between the R and T forms in Met derivatives from that observed for the chemically modified ferrous deoxyHb derivatives; a decrease in band I frequency occurred for T state Met derivatives when compared to the R state.

Nagai *et al.*[35] examined the frequency shifts occurring for the Fe—N_ϵ vibrations in the same chemically modified deoxyhemoglobins as studied by Shelnutt *et al.*[33] Nagai *et al.* found that the Fe—N_ϵ stretching vibration in the R state derivatives occurred ca 4 cm^{-1} higher in frequency than in the T states. These Fe—N_ϵ frequency shifts are at least twice as large as

[79] D. L. Rousseau, J. A. Shelnutt, E. R. Henry, and S. R. Simon, *Nature (London)* **285**, 49 (1980).

any of the RDS frequency shifts detected for the heme macrocyclic vibrational modes by Shelnutt *et al.* The results of Shelnutt *et al.* and Nagai *et al.* could be consistent with a strain in the Fe—N_ϵ bond of T-state deoxy-Hb. The resulting bond change may decrease the electron density in the heme ring, resulting in an increased band I frequency for the T quaternary form.

In this regard, Asher and Schuster's[57,63] study of the fluoride Met derivatives of the isolated α and β subunits and $Mb^{III}F$ indicated that the frequency of the Fe—F stretch increased in the series $\beta^{III}F > \alpha^{III}F > Mb^{III}F$ as the frequencies of some heme macrocyclic vibrations decreased (Fig. 8). However, Asher and Schuster were unable to observe band I frequency shifts because this Raman peak was not enhanced by the excitation wavelengths used in their study.

The recent RDS resonance Raman investigations of the dependence of heme geometry and axial ligand bonding on the globin quaternary structures result in data that either qualitively support strain models for hemoglobin cooperativity or can be interpreted in terms of new mechanisms for differences in heme structure and electron density between the different protein quaternary forms. The order of magnitude increase in the frequency difference resolution by the RDS technique will certainly result in the observation of numerous small spectral differences between different hemoglobins derivatives. The problem remains to correlate these small frequency shifts to structural changes in the heme. This will require extensive characterization of model compounds.

Distal Histidine–Sixth Ligand Interactions

Interactions between the sixth ligand and amino acid side chains may be important as a determinant of the ligand binding affinity of hemoglobin and myoglobin. Although direct hydrogen bonding from the distal histidine to the sixth ligand was suggested by X-ray diffraction measurements[80] of single crystals of $Mb^{III}N_3$, unambiguous characterization of such bonding in solution has been elusive. However, Asher *et al.*[63,81] have used resonance Raman spectroscopy to monitor directly the protonation of the distal histidine at acid pH in $Mb^{III}F$ and $Hb^{III}F$, and the formation of a hydrogen bond to the fluoride ligand. They were also able to relate distal histidine protonation to characteristic absorption spectral changes, and were able to measure distal histidine pK values of 5.1 ($\pm$0.1) and 5.5 ($\pm$0.1) for $Hb^{III}F$ and $Mb^{III}F$, respectively. Figure 15 shows the resonance

[80] L. Stryer, J. C. Kendrew, and H. C. Watson, *J. Mol. Biol.* **8**, 96 (1964).
[81] S. A. Asher, M. L. Adams, and T. M. Schuster, *Biochemistry* **20**, 3339 (1981).

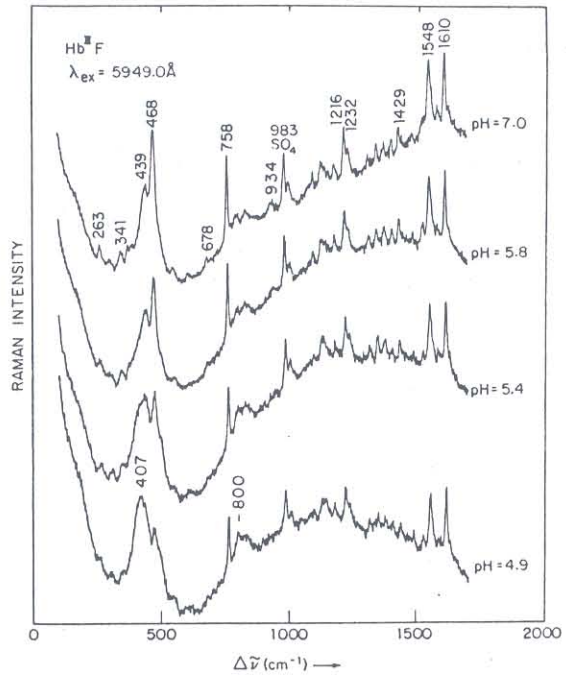

FIG. 15. pH dependence of the resonance Raman spectra of $Hb^{III}F$. The Fe—F stretching vibration occurs at 468 cm^{-1}, whereas the distal histidine–hydrogen bonded Fe—F stretching vibration occurs at 407 cm^{-1}. Excitation wavelength is 5949 Å. From Asher *et al.*[81]

Raman spectra of $Hb^{III}F$ at different pH values. At high pH (>8) the Raman data indicate the presence of $Hb^{III}OH$ (not shown). At lower pH a 60 cm^{-1} shift is observed for the 468 cm^{-1} Fe—F stretch to 407 cm^{-1}. Similar behavior is observed for $Mb^{III}F$, where the Fe—F stretch shifts from 461 cm^{-1} to 399 cm^{-1}. The difference spectra between the different pH samples (Fig. 16) indicate that, as the sample pH decreases, a decrease in intensity occurs for the 468 cm^{-1} peak in conjunction with an increase in intensity for a 407 cm^{-1} peak. The only other changes observed in the Raman spectra is an intensity decrease for the 758 cm^{-1} heme macrocycle stretching vibration and the appearance of a ca 800 cm^{-1} peak that has been assigned to a vibrational overtone of the 407 cm^{-1} peak. $Mb^{III}F$ shows no intensity decrease for the corresponding 760 cm^{-1} peak but does show the presence of a 790 cm^{-1} overtone at pH 5.4.[81] No frequency shifts ($\pm$1 cm^{-1}) are observed for any of the heme macrocyclic modes, indicating that the perturbation of the Fe—F stretching vibration is localized around the fluoride ligand or possibly the iron atom.

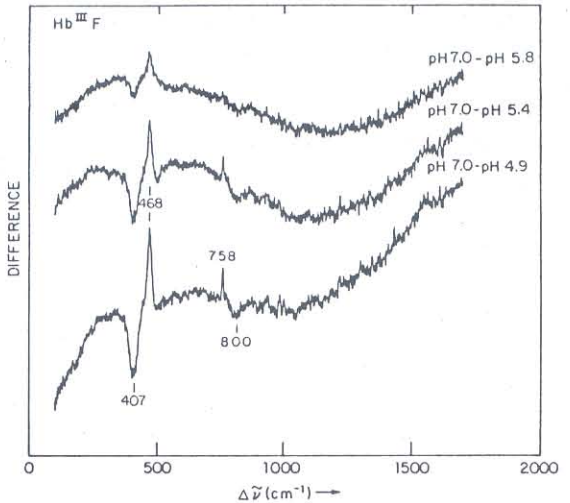

FIG. 16. Raman difference spectra obtained by subtracting individual spectra from the pH 7 spectrum (Fig. 15). From Asher *et al.*[81]

The 60 cm^{-1} frequency shift is interpreted to result from protonation of the distal histidine, which then hydrogen bonds to the fluoride ligand. Since the fluoride ligand is ionically bound, the decrease in the effective fluoride charge results in a bond force constant decrease. This is the opposite behavior to that expected if the proximal histidine protonates; protonation of the proximal histidine would lead to an increased charge at the iron and an increased force constant for the Fe—F bond.

Characteristic absorption spectral changes occur during the titration of the distal histidine. Thus, the pK of the distal histidine can be measured either by resonance Raman or absorption spectral measurements. Figure 17 shows the titration curve measured by both Raman and absorption spectroscopy and indicates representative curves calculated from the Henderson–Hasselbalch equation for different pK values.

It is likely that further resonance Raman measurements of iron–sixth ligand force constants as well as internal ligand vibrations will lead to important data on interactions occurring on the distal side of the heme plane. Comparison of these data with hemoglobins and myoglobins without distal histidines, such as *Glycera* and *Aplysia,* should define the interactions between the distal histidine and the sixth ligand occurring in the physiological pH 7 region. In addition, measurement of amino acid pK values are important monitors of globin tertiary structure because of their sensitivity to amino acid environment.[82] Asher *et al.*[81] measured the distal histidine

[82] J. B. Matthew, G. I. H. Hanania, and F. R. N. Gurd, *Biochemistry* **18,** 1919 (1979) and references therein.

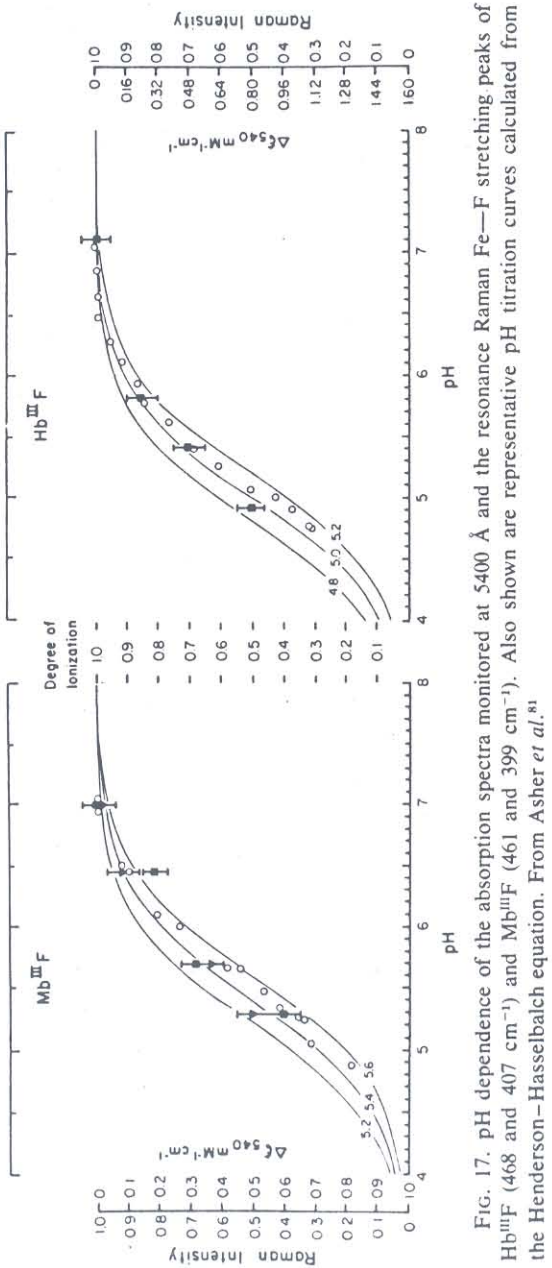

FIG. 17. pH dependence of the absorption spectra monitored at 5400 Å and the resonance Raman Fe—F stretching peaks of Hb^{III}F (468 and 407 cm^{-1}) and Mb^{III}F (461 and 399 cm^{-1}). Also shown are representative pH titration curves calculated from the Henderson–Hasselbalch equation. From Asher *et al.*[81]

pK value in both the R and T forms of $Hb^{III}F$ and observed no change within the resolution of the titration data. From a simple electrostatic model they estimated that any movement of the distal histidine from the fluoride ligand between the R and T quaternary forms is limited to <0.3 Å.

Kinetic Raman Measurements

Resonance Raman measurements of hemoglobin and myoglobin derivatives with continuous laser excitation (CW) probes the equilibrium steady-state heme geometry and iron–ligand bonds. A number of groups have presented kinetic Raman data that may eventually clarify the relationship between the heme geometric changes and tertiary and quaternary protein structural changes.[6–11a]

Friedman and Lyons[7] in 20 nsec–1 msec kinetic resonance Raman spectral studies of carbon monoxy Hb and Mb found that different time domains occur for Raman intensity changes and spectral shifts. The kinetic measurements were interpreted as indicating that different time regimes exist for heme geometric changes, tertiary changes, and quaternary protein structural reorganizations. By using an initial short high-power laser pulse to photolyze the CO ligand, followed at some later time by a probe pulse to excite the resonance Raman spectra, data were obtained in the 20 nsec to 1 msec regime. Since the Soret absorption bands of HbCO and deoxyHb are shifted relative to each other, resonance Raman spectra could be selectively observed for the HbCO and deoxyHb species.

The kinetic Raman study indicated that CO recombination occurs in two time frames as previously observed by kinetic absorption spectral measurements.[83] The geminate recombination lifetime is ca 65 nsec.[7] Little or no geminate recombination was observed for MbCO, suggesting some hemoglobin-specific carbon monoxy binding sites (or potential minima). The fact that ca 50% of the hemoglobin hemes are involved in geminate recombination suggested to Friedman and Lyons[7] that the recombination may be specific for either the α or β subunits.

Kinetic Raman studies[9] of band I frequency shifts in photolyzed HbCO compared to deoxyHb suggested that two time domains exist for structural reorganizations about the heme (Fig. 18). Lyons and Friedman suggested that the tertiary structural changes occur in a time scale of ca 0.8 μsec whereas quaternary structural changes occur in a time scale of ca 200 μsec. If correct, these data present striking evidence in favor of the "trigger mechanism" for the quaternary structural changes associated with cooperativity; in the time domain these data indicate a linkage between heme conformational changes and changes that subsequently propagate through the protein.

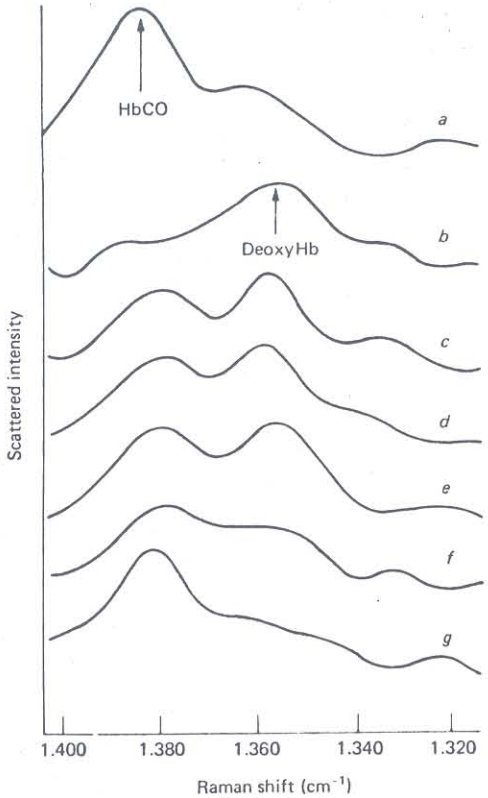

FIG. 18. Resonance Raman spectra of $Hb^{III}CO$ taken at various times after photolysis: a, before photolysis; b, 15 nsec after; c, 100 nsec; d, 1 msec; e, 10 μsec; f, 100 μsec; g, 1 msec. From Friedman and Lyons.[7]

Terner *et al.*[11] have recently studied the kinetic resonance Raman spectra of HbCO in the picosecond and nanosecond time regimes and examined the frequency changes occurring in bands III, IV, and V, which are sensitive to heme core size. They presented evidence for a transient HbCO photolyzed species formed within 20 psec of CO photolysis. Because of the lowered bands III, IV, and V frequencies indicating an expanded heme core size for the transient species compared to normal deoxy Hb, Terner *et al.* suggested that although the iron was high-spin in the photolyzed species it had not yet relaxed to the normal out-of-plane position occurring in deoxyHb.

Because Terner *et al.*[11] and Lyons and Friedman[9] are probing the kinetics of different Raman peaks, it is not clear at this point whether they are examining the same phenomena. However, the importance of these

studies results from the possibility that heme conformational changes involved in ligand binding can be kinetically uncoupled from those involving protein structural reorganizations.

It appears likely that subsequent kinetic studies of other heme vibrational modes, such as the Fe—N_ϵ stretching vibration,[84] may clarify the temporal changes involved in hemoglobin cooperativity. Although much of the free energy of cooperativity may be stored throughout the protein in a form similar to that described by Hopfield's distributed energy model,[85] if the protein structural reorganizations are initiated by changes in bonding at the iron, kinetic measurements of the Fe—N_ϵ bond may show large transient shifts. These localized bond changes, or possibly strains, should subsequently relax and become distributed throughout the protein.

Conclusions

Heme protein resonance Raman spectroscopy has become a relatively routine technique for examining heme conformation and iron–ligand bonding. Instrumentation has been developed that reliably measures <0.1 cm^{-1} frequency shifts between different proteins. Because these frequency shifts can result from heme bond length changes of ca 10^{-4} Å and heme electron density changes of a small fraction of an electron, the sensitivity of the Raman technique to heme geometry and bonding changes exceeds that of other techniques, such as X-ray diffraction or EXAFS. It appears that resonance Raman spectroscopy can directly monitor interactions between the sixth ligand and amino acid side chains on the distal side of the heme plane. The observed empirical correlations between Raman frequency shifts, heme geometry, and globin conformation will continue to be tested by further experiments. These studies will probably result in the elucidation of additional heme-structure sensitive vibrational modes and will clarify the structural sensitivities of bands I–VI.

Until recently, essentially all the resonance Raman measurements in heme proteins have occurred with excitation in the visible spectral region encompassing the α, β, Soret, and various charge-transfer absorption bands. As tunable UV laser sources become more available, resonance Raman measurements will be extended into the unexplored heme UV absorption bands and into the absorption bands of individual aromatic amino acids. These aromatic amino acid studies will be important for the

[83] R. H. Austin, K. W. Beeson, L. Eisenstein, H. Frauenfelder, and I. C. Gunsalus, *Biochemistry* **14**, 5355 (1975).
[84] P. Stein, M. Mitchell, and T. G. Spiro, *J. Am. Chem. Soc.* **102**, 7795 (1980).
[85] J. J. Hopfield, *J. Mol. Biol.* **77**, 207 (1973).

mapping of globin protein structural changes involved in cooperativity. In addition, numerous heme charge-transfer electronic transitions are predicted to exist in the UV.[65] The resonance Raman active vibrational modes observed with UV excitation may include internal vibrational modes of the proximal histidine as well as those of diatomic or triatomic sixth ligands. Studies of these vibrations may elucidate new features of heme–globin interactions. It may also be possible to observe heme macrocycle out-of-plane vibrations, which could be sensitive to the packing of amino acid side chains around the heme.

The years since the first observation of the resonance Raman spectrum of hemoglobin have resulted in numerous incisive, not necessarily conclusive, glimpses of heme geometry. As work progresses the focus is expected to extend further from the heme, possibly to globin aromatic amino acids at sites distant from the heme macrocycle.

Acknowledgments

I wish gratefully to acknowledge helpful conversations with Dr. Joel Friedman, Dr. Dennis Rousseau, Professor Thomas Spiro, and Professor Nai-Teng Yu and to thank them for permitting me the use of figures from their work. I would also like to thank my collaborators, especially Todd Schuster from the Biological Sciences Group of the University of Connecticut, Storrs. I am grateful also to Professor Peter Pershan for his hospitality while I was a postdoctoral fellow in his laboratory and for making available facilities to build the resonance Raman spectrometer used to obtain many of the measurements reported in this review.